

# Player of Games

Martin Schmid	Matej Moravčík	Neil Burch	Rudolf Kadlec
Josh Davidson	Kevin Waugh	Nolan Bard	Finbarr Timbers
Marc Lanctot	Zach Holland	Elnaz Davoodi	Alden Christianson

Michael Bowling

DeepMind\*

## Abstract

Games have a long history of serving as a benchmark for progress in artificial intelligence. Recently, approaches using search and learning have shown strong performance across a set of perfect information games, and approaches using game-theoretic reasoning and learning have shown strong performance for specific imperfect information poker variants. We introduce Player of Games, a general-purpose algorithm that unifies previous approaches, combining guided search, self-play learning, and game-theoretic reasoning. Player of Games is the first algorithm to achieve strong empirical performance in large perfect and imperfect information games — an important step towards truly general algorithms for arbitrary environments. We prove that Player of Games is sound, converging to perfect play as available computation time and approximation capacity increases. Player of Games reaches strong performance in chess and Go, beats the strongest openly available agent in heads-up no-limit Texas hold’em poker (Slumbot), and defeats the state-of-the-art agent in Scotland Yard, an imperfect information game that illustrates the value of guided search, learning, and game-theoretic reasoning.

## 1 Introduction

In the 1950s, Arthur L. Samuel developed a Checkers-playing program that employed what is now called minimax search (with alpha-beta pruning) and “rote learning” to improve its evaluation function via self-play [62]. This investigation inspired many others, and ultimately Samuel co-founded the field of artificial intelligence [61] and popularized the term “machine learning”. A few years ago, the world witnessed a computer program defeat a long-standing professional at the game of Go [70]. AlphaGo also combined learning and search. Many similar achievements happened in between such as the race for super-human chess leading to DeepBlue [17] and TD-Gammon teaching itself to play master-level performance in Backgammon through self-play [82], continuing the tradition of using games as canonical markers of mainstream progress across the field.

Throughout the stream of successes, there is an important common element: the focus on a single game. Indeed, DeepBlue could not play Go, and Samuel’s program could not play chess. Likewise, AlphaGo could not play chess; however its successor AlphaZero [71] could, and did. AlphaZero demonstrated that a single algorithm could master three different perfect information games using a simplification of AlphaGo’s approach, and with minimal human knowledge. Despite this success, AlphaZero could not play poker, and the extension to imperfect information games was unclear.

Meanwhile, approaches taken to achieve super-human poker AI were significantly different. Strong poker play has relied on *game-theoretic reasoning* to ensure that private information is concealed effectively. Initially, super-human poker agents were based primarily on computing approximate Nash equilibria offline [37]. Search was then added and proved to be a crucial ingredient to achieve super-human success in no-limit variants [55, 11, 12]. Training for other large games have also been inspired by game-theoretic reasoning and search, such as Hanabi [4, 44], The Resistance [69], Bridge [49], AlphaStar [83], and (no-press) Diplomacy [2, 25, 3]. Here again, however, despite remarkable success: each advance was still on a single game, with some clear uses of domain-specific knowledge and structure to reach strong performance.

In this paper, we introduce Player of Games (PoG), a new algorithm that generalizes the class of games in which strong performance can be achieved using self-play learning, search, and game-

---

\*Contact author: [bowlingm@deepmind.com](mailto:bowlingm@deepmind.com).

theoretic reasoning. PoG uses growing-tree counterfactual regret minimization (GT-CFR): an anytime local search that builds subgames non-uniformly, expanding the tree toward the most relevant future states while iteratively refining values and policies. In addition, PoG employs sound self-play: a learning procedure that trains value-and-policy networks using both game outcomes *and* recursive sub-searches applied to situations that arose in previous searches.

Player of Games is the first algorithm to achieve strong performance in challenge domains with both perfect *and* imperfect information — an important step towards truly general algorithms that can learn in arbitrary environments. Applications of traditional search suffer well-known problems in imperfect information games [61]. Evaluation has remained focused on single domains (e.g. poker) despite recent progress toward sound search in imperfect information games [55, 10, 84]. Player of Games fills this gap, using a single algorithm with minimal domain-specific knowledge. Its search is sound [84] across these fundamentally different game types: it is guaranteed to find an approximate Nash equilibrium by re-solving subgames to remain consistent during online play, and yielding low exploitability in practice in small games where exploitability is computable. PoG demonstrates strong performance across four different games: two perfect information (chess and Go) and two imperfect information (poker and Scotland Yard). Finally, unlike poker, Scotland Yard has significantly longer search horizons and game lengths, requiring long-term planning.

## 2 Background and Terminology

We start with necessary background and notation to describe the main algorithm and results. We relate our algorithm to other approaches in Section 5. Here, we give a concise introduction to necessary concepts, which are based on the Factored-Observation Stochastic Games (FOSG) formalism. For further details on the formalism, see [40, 64].

A game between two players starts in a specific **world state**  $w^{init}$  and proceeds to the successor world states  $w \in \mathcal{W}$  as a result of players choosing actions  $a \in \mathcal{A}$  until the game is over when a terminal state is reached. At any world state  $w$ , we will use the notation  $\mathcal{A}(w) \subseteq \mathcal{A}$  to refer to those actions that are available, or legal, in world state  $w$ . Sequences of actions taken along the course of the game are called **histories** and denoted  $h \in \mathcal{H}$ , with  $h' \sqsubseteq h$  denoting a prefix history (subsequence). At terminal histories,  $z \in \mathcal{H}$ , each player  $i$  receives a utility  $u_i(z)$ .

An **information state** (private state) is a state with respect to one player’s information. Specifically,  $s_i \in \mathcal{S}_i$  for player  $i$  is a set of histories that are indistinguishable due to missing information. A simple example is a specific decision point in poker where player  $i$  does not know the opponent’s private cards; the histories in the information state are different only in the chance event outcomes that determine the opponent’s private cards, since everything else is public knowledge. A player  $i$  plays a **policy**  $\pi_i : \mathcal{S}_i \rightarrow \Delta(\mathcal{A})$ , where  $\Delta(\mathcal{A})$  denotes the set of probability distributions over actions  $\mathcal{A}$ . The goal of each player is to find a policy that maximizes their own expected utility.

Every time a player takes an action, each player gets a **private observation**  $\mathcal{O}_{priv(i)}(w, a, w')$  and a **public observation**  $\mathcal{O}_{pub}(w, a, w')$  as a result of applying action  $a$ , changing the game’s

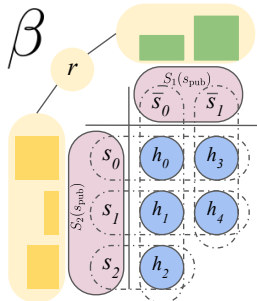


Figure 1: An example structure of public belief state  $\beta = (s_{\text{pub}}, r)$ .  $s_{\text{pub}}$  translates to two sets of information states, one for player 1,  $\mathcal{S}_1(s_{\text{pub}}) = \{\bar{s}_0, \bar{s}_1\}$ , and one for player 2,  $\mathcal{S}_2(s_{\text{pub}}) = \{s_0, s_1, s_2\}$ . Each information state includes different partitions of possible histories. Finally  $r$  contains reach probabilities for information states for both players.

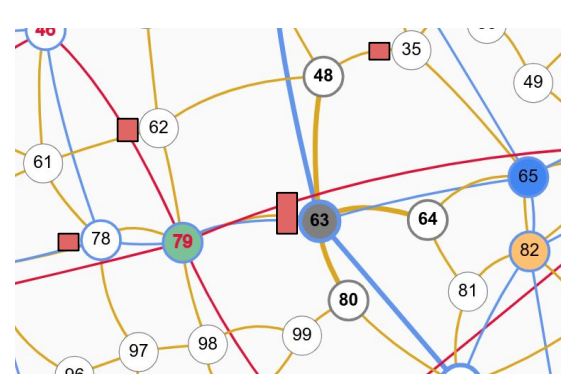


Figure 2: A depiction of a public belief state in Scotland Yard: circles are locations, edges are transportation links, and red bars indicate beliefs of the private (unrevealed) information state of Mr. X’s location.

state from  $w$  to  $w'$ . A **public state**  $s_{\text{pub}} = s_{\text{pub}}(h) \in \mathcal{S}_{\text{pub}}$  is the sequence of public observations encountered along the history  $h$ . For example, a public state in Texas hold'em poker is represented by initial public information (stack sizes and antes), the betting history, and any publicly revealed board cards. Let  $\mathcal{S}_i(s_{\text{pub}})$  be the set of possible information states for player  $i$  given  $s_{\text{pub}}$ : each information state  $s_i \in \mathcal{S}_i(s_{\text{pub}})$  is consistent with public observations in  $s_{\text{pub}}$  but has different sequences of private observations. For example, in poker the information states would contain the private cards of player  $i$ . A full example of a FOSG is shown in Appendix A.

A **public belief state**  $\beta = (s_{\text{pub}}, r)$ , where the **range** (or beliefs)  $r \in \Delta(\mathcal{S}_1(s_{\text{pub}})) \times \Delta(\mathcal{S}_2(s_{\text{pub}}))$  is a pair of distributions over possible information states for both players representing the beliefs over information states in  $s_{\text{pub}}$ . A basic depiction of the various components of a public belief state is depicted in Figure 1. In the game of Scotland Yard, for instance, the information states correspond to the location of the evader (Mr. X). A specific example is shown in Figure 2. The true location of the evader is hidden but can be one of four different locations, and detectives have a stronger suspicion that the evader is on location 63 than 35, 62, or 78. In Scotland Yard, one of the distributions in  $r$  is a point mass because the detectives do not have any private information hidden from Mr. X.

Suppose players use joint policy  $\pi = (\pi_1, \pi_2)$ . Denote the expected utility to player to player  $i$  as  $u_i(\pi_1, \pi_2)$  and  $-i$  as the opponent of player  $i$ . A **best response** policy is any policy  $\pi_i^b$  that achieves maximal utility against some  $\pi_{-i}$ :  $u_i(\pi_i^b, \pi_{-i}) = \max_{\pi'_i} u_i(\pi'_i, \pi_{-i})$ . A joint policy  $\pi$  is a **Nash equilibrium** if and only if  $\pi_1$  is a best response to  $\pi_2$  and  $\pi_2$  is a best response to  $\pi_1$ . There are also approximate equilibria:  $\pi$  is an  $\epsilon$ -**Nash equilibrium** if and only if  $u_i(\pi_i^b, \pi_{-i}) - u_i(\pi_i, \pi_{-i}) \leq \epsilon$  for all players  $i$ . In two-player zero-sum games, Nash equilibria are optimal because they maximize worst-case utility guarantees for both players. Also, equilibrium strategies are *interchangeable*: if  $\pi^A$  and  $\pi^B$  are Nash equilibria, then  $(\pi_1^A, \pi_2^B)$  and  $(\pi_1^B, \pi_2^A)$  are also both equilibria. Hence, the agent's goal is to compute one such optimal (or approximately optimal) equilibrium strategy.

## 2.1 Tree Search and Machine Learning

The first major milestones in the field of AI were obtained by efficient search techniques inspired by the minimax theorem [62, 17]. In a two-player zero-sum game with perfect information, the approach uses depth-limited search starting from the current world state  $w_t$ , along with a heuristic evaluation function to estimate value of the states beyond the depth limit,  $h(w_{t+d})$  and game-theoretic reasoning to back up values [38]. Researchers developed significant search enhancements [52, 63] which greatly improved performance, leading to IBM's super-human DeepBlue chess program [17].

This classical approach was, however, unable to achieve super-human performance in Go, which has significantly larger branching factor and state space complexity than chess. Prompted by the challenge of Go [24], researchers proposed Monte Carlo tree search (MCTS) [39, 18]. Unlike minimax search, MCTS builds trees via simulations, starting with an empty tree rooted by  $w_t$  and expanding the tree by adding the first state encountered in simulated trajectories not currently in the tree, and finally estimating values from rollouts to the end of the game. MCTS led to significantly stronger play in Go and other games [14], attaining 6 dan amateur level in Go. However, heuristics in the form of domain knowledge were still necessary to achieve these milestones.

In AlphaGo [70], value functions and policies are incorporated, learned initially from human expert data, and then improved via self-play. A deep network approximates the value function and a prior policy helps guide the selection of actions during the tree search. The approach was the first to achieve super-human level play in Go [70]. AlphaGo Zero removed the initial training from human data and Go-specific features [72]. AlphaZero reached state-of-the-art performance in Chess and Shogi as well as Go, using minimal domain knowledge [71].

POG, like AlphaZero, combines search and learning from self-play, using minimal domain knowledge. Unlike MCTS, however, which is not sound for imperfect information games, POG's search algorithm is based on counterfactual regret minimization and is sound for both perfect and imperfect information games.

## 2.2 Game-Theoretic Reasoning and Counterfactual Regret Minimization

In imperfect information games, the choice of strategies that arise from hidden information can be crucial to determining each player's expected rewards. Simply playing too predictably can be problematic: in the classic example game of Rock, Paper, Scissors, the only thing a player does not know is the choice of the opponent's action, however this information fully determines their achievable reward. A player choosing to always play one action (e.g. rock) can be easily beaten by

another playing the best response (e.g. paper). The Nash equilibrium plays each action with equal probability, which minimizes the benefit of any particular counter-strategy. Similarly, in poker, knowing the opponent’s cards or their strategy could yield significantly higher expected reward, and in Scotland Yard, players have a higher chance of catching the evader if their current location is known. In these examples, players can exploit any knowledge of hidden information to play the counter-strategy resulting in higher reward. Hence, to avoid being exploited, players must act in a way that does not reveal their own private information. We call this general behavior **game-theoretic reasoning** because it emerges as the result of computing (approximate) minimax-optimal strategies. Game-theoretic reasoning has been paramount to the success of competitive poker AI over the last 20 years.

One algorithm for computing approximate optimal strategies is counterfactual regret minimization (CFR) [86]. CFR is a self-play algorithm that produces policy iterates  $\pi_i^t(s)$  for each player  $i$  at each of their information states  $s$  in a way that minimizes long-term average regret. As a result, the average policy over  $T$  iterations,  $\bar{\pi}^T$ , employed by CFR in self-play converges to an  $\epsilon$ -Nash equilibrium, at a rate of  $O(1/\sqrt{T})$ . At each iteration,  $t$ , counterfactual values  $v_i(s, a)$  are computed for each action  $a \in \mathcal{A}(s)$  and immediate regrets for not playing  $a$ ,  $r(s, a) = v_i(s, a) - \sum_{a \in \mathcal{A}(s)} \pi(s, a) v_i(s, a)$ , are computed and tabulated in a cumulative regret table storing  $R^T(s, a) = \sum_{t=1}^T r^t(s, a)$ . A new policy is computed using regret-matching [27]:  $\pi^{t+1}(s) = \frac{[R^t(s, a)]^+}{\sum_a [R^t(s, a)]^+}$ , where  $[x]^+ = \max(x, 0)$ , and reset to uniform if all the regrets are non-positive.

CFR<sup>+</sup> [79] is a successor of CFR that played a key role in fully solving the game of heads-up limit hold’em poker, the largest imperfect information game to be solved to date [6]. A main component of CFR<sup>+</sup> is a different policy update mechanism, regret-matching<sup>+</sup>, which defines cumulative values slightly differently:  $Q^t(s, a) = (Q^{t-1}(s, a) + r^t(s, a))^+$ , and  $\pi^{t+1}(s, a) = Q^t(s, a) / \sum_b Q^t(s, b)$ .

A common form of CFR (or CFR<sup>+</sup>) is one that traverses the **public tree**, rather than the classical extensive-form game tree. Quantities required to compute counterfactual values, such as each player’s probabilities of reaching each information state under their policy (called their **range**) are maintained as beliefs. Finally, leaf nodes can be evaluated directly using the ranges, chance probabilities, and utilities (often more efficiently [36]).

### 2.3 Imperfect Information Search, Decomposition, and Re-Solving

Solution concepts like Nash equilibria and minimax are defined over joint *policies*. The policy is fixed during play. Search could instead be described as a process, which might return different action distributions at subsequent visits to the same state. In search-based decision-making, new solutions are computed at the decision-time. Each state could depend on the past game-play, time limits, and samples of stochastic (chance) events, which introduces important subtleties such as solution compatibility across different searches [84].

CFR has been traditionally used as a solver, computing entire policies via self-play. Each iteration traverses the entire game tree, recursively computing values for information states from other values at subgames deeper in the tree. Suppose one wanted a policy for a part of the game up to some depth  $d > 0$ . If there was an oracle to compute the values at depth  $d$ , then each iteration of CFR could be run to depth  $d$  and query the oracle to return the values. As a result, the policies would not be available at depths  $d' > d$ . Summarizing the policies below depth  $d$  by a set of values which can be used to reconstruct policies at depth  $d$  and beyond is the basis of **decomposition** in imperfect information games [15]. A **subgame** in an imperfect information game is a game rooted at a public state  $s_{\text{pub}}$ . In order for a subgame to be a proper game, it is paired with a belief distribution  $r$  over initial information states,  $s \in \mathcal{S}_i(s_{\text{pub}})$ . This is a strict generalization of subgames in perfect information games, where every public state has exactly one information state (which is, in fact, no longer private as a result) and a single belief with probability 1.

Subgame decomposition has been a crucial component of most recent developments of poker AI that scale to large games such as no-limit Texas hold’em [55, 11, 12, 7]. Subgame decomposition enables local search to refine the policy during play analogously to the classical search algorithms in perfect information games and traditional Bellman-style bootstrapping to learn value functions [55, 69, 85, 7]. Specifically, a **counterfactual value network** (CVN) represented by parameters  $\theta$  encodes the value function  $\mathbf{v}_\theta(\beta) = \{v_i(s_i)\}_{s_i \in \mathcal{S}_i(s_{\text{pub}}), i \in \{1, 2\}}$ , where  $\beta$  includes player’s beliefs over information states for the public information at  $s_{\text{pub}}$ . The function  $\mathbf{v}_\theta$  can then be used in place of the oracles mentioned above to summarize values of the subtrees below  $s_{\text{pub}}$ . An example of depth-limited CFR solver using decomposition is shown in Figure 3.

**Safe re-solving** is a technique that generates subgame policies from only summary information

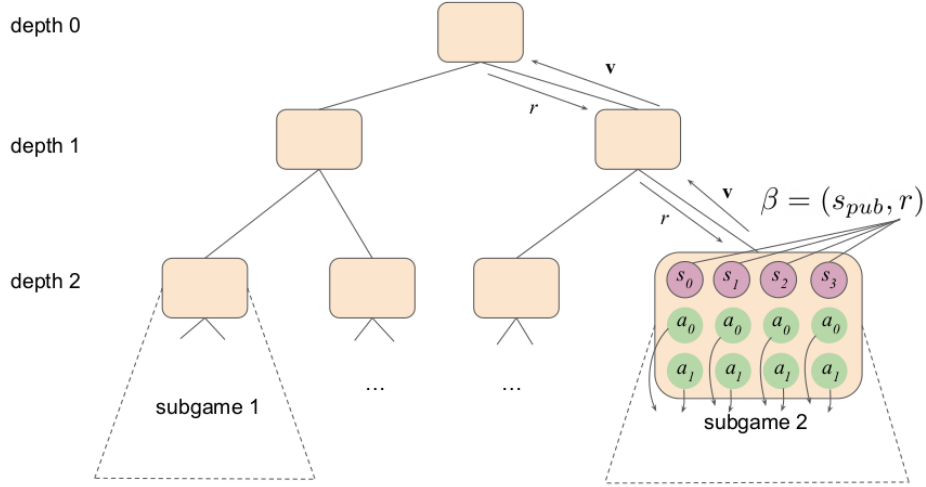


Figure 3: An example game with two specific subgames shown. Standard CFR would require traversing all the subgames. Depth-limited CFR decomposes the solve into running down to depth  $d = 2$  and using  $\mathbf{v} = \mathbf{v}_\theta(\beta)$  to represent the second subgame’s values. On the downward pass, ranges  $r$  are formed from policy reach probabilities. Values are passed back up to tabulate accumulating regrets. Re-solving a subgame would require construction of an auxiliary game [15] (not shown).

of a previous (approximate) solution: a player’s range and their opponent’s counterfactual values. This is done by constructing an auxiliary game with specific constraints. The subgame policies in the auxiliary game are generated in a way that preserves the exploitability guarantees of the original solve, so they can replace the original policies in the subgame. Thorough examples of the auxiliary game construction are found in [15] and [10, Section 4.1].

**Continual re-solving** is an analogue of classical game search, adapted to imperfect information games, that uses repeated applications of safe re-solving to play an episode of a game [55]. It starts by solving a depth-limited game tree rooted at the beginning of the game, and search is a re-solving step. As the game progresses, for every subsequent decision at some information state  $s_i$ , continual re-solving will refine the current strategy by re-solving at  $s_i$ . Like other search methods, it is using additional computation to more thoroughly explore a specific situation encountered by the player. The continual re-solving method of [55] uses a few properties of poker which are not found in other games like Scotland Yard, so we use a more general re-solving method which can be applied to a broader class of games. We discuss the details of this more general re-solving variant in Appendix B.1.

### 3 Player of Games

We now describe our main algorithm. As PoG has several components, we describe them each individually first, and then describe how they are all combined toward the end of the section.

For clarity, many of the details (including full pseudocode) are presented in Appendix B.

#### 3.1 Counterfactual Value-and-Policy Networks

The first major component of PoG is a **counterfactual value-and-policy network** (CVPN) with parameters  $\theta$ , depicted in Figure 4. These parameters represent a function  $f_\theta(\beta) = (\mathbf{v}, \mathbf{p})$ , where outputs  $\mathbf{v}$  are counterfactual values (one per information state per player), and *prior policies*  $\mathbf{p}$ , one per information state for the acting player, in the public state  $s_{\text{pub}}(h)$  at some history of play  $h$ .

In our experiments, we use standard feed-forward networks and residual networks. The details of the architecture are described in Section B.3.

#### 3.2 Search via Growing-Tree CFR

Growing-tree CFR (GT-CFR) is a new algorithm that runs a CFR variant on a public game tree that is incrementally grown over time. GT-CFR starts with an initial tree,  $\mathcal{L}^0$ , containing  $\beta$  and all of its child public states. Then each iteration,  $t$ , of GT-CFR consists of two phases:

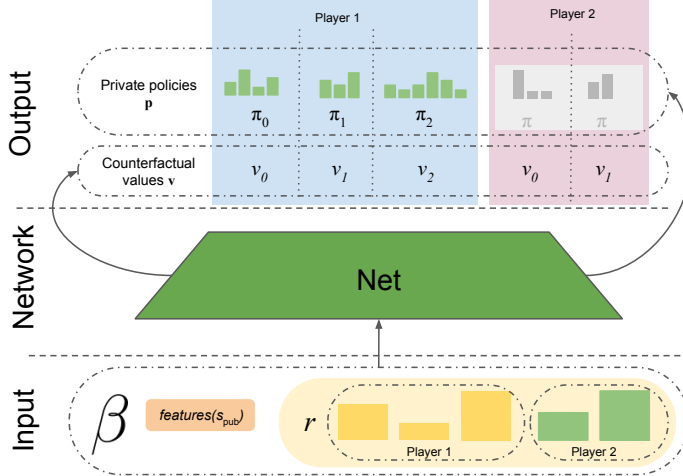


Figure 4: A counterfactual value-and-policy network (CVPN). Each query,  $\beta$ , to the network includes beliefs  $r$  and an encoding of  $s_{\text{pub}}$  to get the counterfactual values  $\mathbf{v}$  for both players and policies  $\mathbf{p}$  for the acting player in each information state  $s_i \in s_{\text{pub}}(h)$ , producing outputs  $f_{\theta}$ . Since players may have different actions spaces (as in *e.g.* Scotland Yard) there are two sets of policy outputs: one for each player, and  $\mathbf{p}$  refers to the one for the acting player at  $s_{\text{pub}}$  only (depicted as player 1 in this diagram by greying out player 2’s policy output).

1. The **regret update phase** (described in detail in subsection 3.2.1) runs several public tree CFR updates on the current tree  $\mathcal{L}^t$ .
2. The **expansion phase** (described in detail in subsection 3.2.2) expands  $\mathcal{L}^t$  by adding new public states via simulation-based expansion trajectories, producing a new larger tree  $\mathcal{L}^{t+1}$ .

When reporting the results we use the notation  $\text{PoG}(s, c)$  for PoG running GT-CFR with  $s$  total expansion simulations, and  $c$  expansion simulations per regret update phase, so the total number of GT-CFR iterations is then  $\frac{s}{\lceil c \rceil}$ . For example,  $\text{PoG}(8000, 10)$  refers to 8000 expansion simulations at 10 expansions per regret update (800 GT-CFR iterations). The  $c$  can be fractional, so *e.g.* 0.1 indicates a new node every 10 regret update phases. Figure 5 depicts the whole GT-CFR cycle. We chose this specific notation to directly compare total expansion simulations,  $s$ , to AlphaZero.

### 3.2.1 The Regret Update Phase of Growing-Tree CFR

The regret update phase runs  $\lceil \frac{1}{c} \rceil$  updates (iterations) of public tree CFR on  $\mathcal{L}^t$  using simultaneous updates, regret-matching<sup>+</sup>, and linearly-weighted policy averaging [79]. At public tree leaf nodes, a **query** is made to the CVPN at belief state  $\beta'$ , whose values  $f_{\theta}(\beta') = (\mathbf{v}, \mathbf{p})$  are used as estimates of counterfactual values for the public subgame rooted at  $\beta'$ .

### 3.2.2 The Expansion Phase of Growing-Tree CFR

In the expansion phase, new public tree nodes are added to  $\mathcal{L}$ . Search statistics, initially empty, are maintained over information states  $s_i$ , accumulated over all expansion phases within the same search. At the start of each simulation, a information state  $s_i$  is sampled from the beliefs in  $\beta_{\text{root}}$ . Then, a world state  $w_{\text{root}}$  is sampled from  $s_i$ , with associated history  $h_{\text{root}}$ . Actions are selected according to a mixed policy that takes into account learned values (via  $\pi_{\text{PUCT}}(s_i(h))$ ) as well as the currently active policy ( $\pi_{\text{CFR}}(s_i(h))$ ) from search:  $\pi_{\text{select}}(s_i(h)) = \frac{1}{2}\pi_{\text{PUCT}}(s_i(h)) + \frac{1}{2}\pi_{\text{CFR}}(s_i(h))$ . The first policy is determined by PUCT [70] using counterfactual values  $v_i(s_i, a)$  normalized by the sum of the opponent’s reach probability at  $s_i$  to resemble state-conditional action values, and the prior policy  $\mathbf{p}$  obtained from the queries. The second is simply CFR’s current policy at  $s_i(h)$ . As soon as the simulation encounters a information state  $s_i \in s_{\text{pub}}$  such that  $s_{\text{pub}} \notin \mathcal{L}$ , the simulation ends,  $s_{\text{pub}}$  is added to  $\mathcal{L}$ , and visit counts are updated along nodes visited during the trajectory. Similarly to AlphaZero [71], virtual losses [68] are added to the PUCT statistics when doing  $\lceil c \rceil$  simulations inside one GT-CFR iteration.

AlphaZero always expands a single action/node at the end of the iteration (the action with the highest UCB score). Optimal policies in perfect information games can be deterministic and thus expanding a single action/node is sufficient. In imperfect information games, optimal policies might

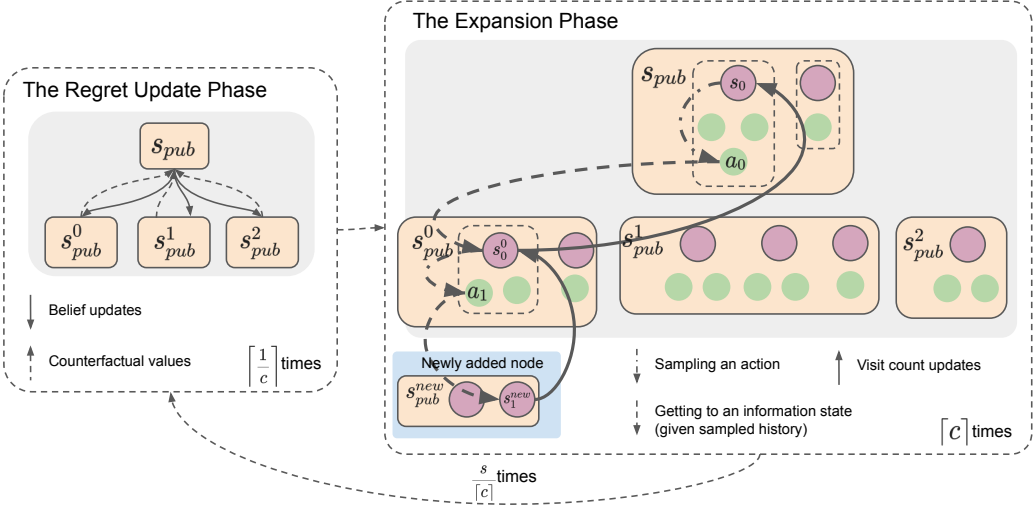


Figure 5: Overview of phases in one iteration of Growing-Tree CFR. The regret update phase propagates beliefs down the tree, obtains counterfactual values from the CPVN at leaf nodes (or from the environment at terminals), and passes back counterfactual values to apply the CFR update. The expansion phase simulates a trajectory from the root to leaf, adding public states to the tree. In this case the trajectory starts in the public belief state  $s_{pub}$  by sampling the information state  $s_0$ , after that the sampled action  $a_0$  leads to the information state  $s_0^0$  in public state  $s_{pub}^0$  finally the action  $a_1$  leads to a new public state that is added to the tree.

be stochastic, having non-zero probability over multiple actions (the number of such actions is then referred to as the support size). There is a direct link between the level of uncertainty in the game (in terms of information states per public state) and the support size [66]. In other words, the number of actions potentially required by an optimal policy is a function of the number of information states per public state, and we refer to this number as the minimum support size  $k$ . Rather than expanding a single action, POG thus expands the top  $k$  actions as ranked by the prior. All the public states corresponding to the expanded actions are then added to the tree (together with all the actions leading to those public states). When POG expands a previously expanded node, only a single action is additionally expanded as the minimum support size requirement is already satisfied. Note that for perfect information games, the expansion acts the same as AlphaZero as the support size  $k = 1$  and thus a single action having the highest prior is added.

### 3.2.3 Convergence Guarantees

Growing the tree in GT-CFR allows the search to selectively focus on parts of the space that are important for local decisions. Starting with a small tree and adding nodes over time does not have an additional cost in terms of convergence:

**Theorem 1.** *Let  $\mathcal{L}^t$  be the public tree at time  $t$ . Assume public states are never removed from the lookahead tree, so  $\mathcal{L}^t \subseteq \mathcal{L}^{t+1}$ . For any given tree  $\mathcal{L}$ , let  $\mathcal{N}(\mathcal{L})$  be the interior of the tree: all non-leaf, non-terminal public states where GT-CFR generates a policy. Let  $\mathcal{F}(\mathcal{L})$  be the frontier of  $\mathcal{L}$ , containing the non-terminal leaves where GT-CFR uses  $\epsilon$ -noisy estimates of counterfactual values. Let  $U$  be the maximum difference in counterfactual value between any two strategies, at any information state, and  $A$  be the maximum number of actions at any information state. Then, the regret at iteration  $T$  for player  $i$  is bounded:*

$$R_i^{T,\text{full}} \leq \sum_{t=1}^T |\mathcal{F}(\mathcal{L}^t)|\epsilon + \sum_{s_{pub} \in \mathcal{N}(\mathcal{L}^T)} |\mathcal{S}_i(s_{pub})|U\sqrt{AT}$$

The regret  $R_i^{T,\text{full}}$  in Theorem 1 is the gap in performance between GT-CFR iterations and any possible strategy. Theorem 1 shows that the average policy returned by GT-CFR converges towards a Nash equilibrium at a rate of  $1/\sqrt{T}$ , but with some minimum exploitability due to  $\epsilon$ -error in the value function. There is also no additional cost when using GT-CFR as the game-solving algorithm for each re-solving search step in continual re-solving:

**Theorem 2.** Assume we have played a game using continual re-solving, with one initial solve and  $D$  re-solving steps. Each solving or re-solving step finds an approximate Nash equilibrium through  $T$  iterations of GT-CFR using an  $\epsilon$ -noisy value function, public states are never removed from the lookahead tree, the maximum interior size  $\sum_{s_{\text{pub}} \in \mathcal{N}(\mathcal{L}^T)} |\mathcal{S}_i(s_{\text{pub}})|$  of all lookahead trees is bounded by  $N$ , the sum of frontier sizes across all lookahead trees is bounded by  $F$ , the maximum number of actions at any information sets is  $A$ , and the maximum difference in values between any two strategies is  $U$ . The exploitability of the final strategy is then bounded by  $(5D + 2) \left( F\epsilon + NU\sqrt{\frac{A}{T}} \right)$ .

Theorem 2 is similar to Theorem 1 of [55], adapted to GT-CFR and using a more detailed error model which can more accurately describe value functions trained on approximate equilibrium strategies. It shows that continual re-solving with GT-CFR has the general properties we might desire: exploitability decreases with more computation time and decreasing value function error, and does not grow uncontrollably with game length. Proofs of the theorems are presented in Appendix E.

### 3.3 Data Generation via Sound Self-play

Player of Games generates episodes of data in self-play by running searches at each decision point. Each episode starts at the initial history  $h_0$  corresponding to the start of the game, and produces a sequence of histories  $(h_0, h_1, \dots)$ . At time  $t$ , the agent runs a local search and then selects an action  $a_t$ , and the next history  $h_{t+1}$  is obtained from the environment by taking action  $a_t$  at  $h_t$ . Data for training the CVPN is collected via resulting trajectories and the individual searches.

When generating data for training the CVPN, it is important that searches performed at different public states be consistent with both the CVPN represented by  $\theta$  and with searches made at previous public states along the same trajectory (e.g. two searches should not be computing parts of two different optimal policies). This is a critical requirement for sound search [15, 55, 84], and we refer to the process of a sound search algorithm generating data in self-play as **sound self-play**.

To achieve sound self-play, searches performed during data generation run GT-CFR on the standard safe resolving auxiliary game (as described in Section 2.3). The auxiliary game includes an option at the initial decision for the opponent to decide to enter the subgame, or take the alternative values returned by  $f_\theta(\beta)$ . For a detailed construction of this resolving process, see Section B.1.

### 3.4 Training Process

The quality of the policies produced by GT-CFR and data generated by sound self-play depends critically on the values returned by the CVPN. Hence, it is important for the estimates to be accurate in order to produce high-performance searches and generate high-quality data. In this subsection, we describe the procedure we use to train the CVPN. The process is summarized in Figure 6.

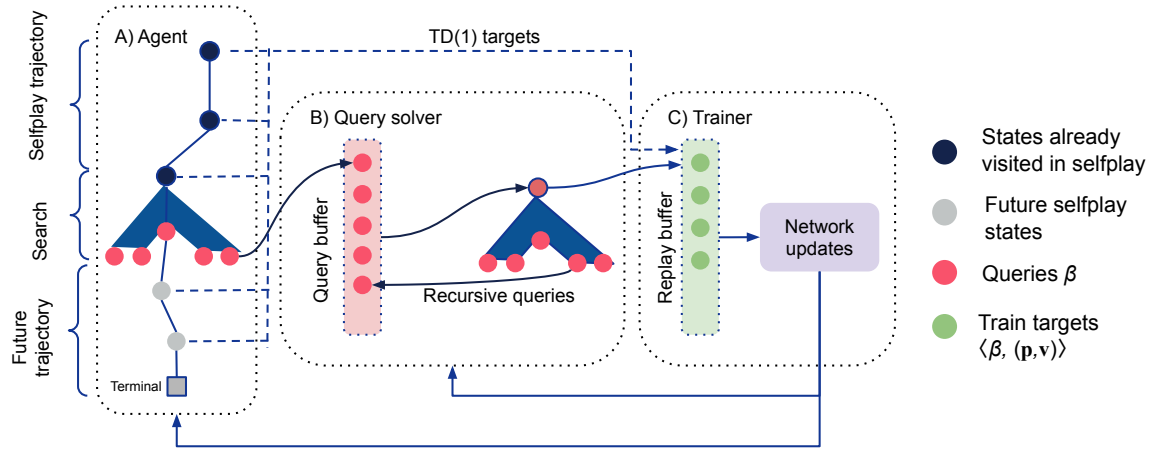


Figure 6: POG Training Process. Actors collect data via sound self-play and trainers run separately over a distributed network. (A) Each search produces a number of CVPN **queries** with input  $\beta$ . (B) Queries are added to a query buffer and subsequently solved by a **solver** that studies the situation more closely via another invocation of GT-CFR. During solving, new recursive queries might be added back to the query buffer; separately the network is (C) trained on minibatches sampled from the replay buffer to predict values and policy targets computed by the solver.

### 3.4.1 Query Collection

As described in sections 3.2 and 3.3, episodes are generated by each player running searches of GT-CFR from the current public state. Each search produces a number of network queries from public tree leaf nodes  $\beta$  (depicted as pink nodes in Figure 6).

The training process improves the CVPN via supervised learning. Values are trained using Huber loss [32] based on value targets and the policy loss is cross entropy with respect to a target policy. Value and policy targets are added to a sliding window data set of training data that is used to train the CVPN concurrently. The CVPN is updated asynchronously on the actors during training.

### 3.4.2 Computing Training Targets

Policy targets are assembled from the searches started at public states along the main line of episodes (the histories reached in self-play) generated by sound self-play described in 3.3. Specifically, they are the output policies for all information states within the root public state, computed in the regret update phase of GT-CFR.

Value targets are obtained in two different ways. Firstly, the outcome of the game is used as a (TD(1)) value target for states along the main line of episodes generated by sound self-play. Secondly, value targets are also obtained by bootstrapping: running an instance of GT-CFR from subgames rooted at input queries. In principle, any solver could be used because any subgame rooted at  $\beta$  has well-defined values. Thus, this step acts much like a policy improvement operator via decomposition described in Section 2.3. Specifically, the value targets are the final counterfactual values after  $T$  iterations of GT-CFR for all the information states within the public state that initiated the search. The specific way that the different value targets are assigned is described by the pseudocode in Section B.5 and determined by a hyperparameter described in Section B.4.

### 3.4.3 Recursive Queries

While the solver is computing targets for a query, it is also generating more queries itself by running GT-CFR. Some of these **recursive queries** are also added to the buffer for future solving. As a result, at any given time the buffer may include queries generated by search in the main self-play game or by solver-generated queries off the main line. To ensure that the buffer is not dominated by recursive queries, we set the probability of adding a new recursive query to less than 1 (in our experiments, the value is typically 0.1 or 0.2; see Section B.4 for the exact values).

### 3.4.4 Consistency of Training Process

One natural question is whether, or under what circumstances, the training process could ensure convergence to the optimal values? The answer is positive: the training process converges to the optimal values, asymptotically, as  $T \rightarrow \infty$  and with very large (exponential) memory.

Informally, imagine an oracle function  $f(\beta)$  that can simply memorize the values and policy for the particular  $\beta$  similar to a tabular value or policy iteration algorithm except with continuous keys. For any subgame rooted at some  $\beta$  with a depth of 1 (every action leads to terminal states), the values and policies can be computed and stored for  $\beta$  after  $T$  iterations of the solver. This can then be applied inductively: since CFR is deterministic, for any subgame on the first iteration of GT-CFR, a finite number of queries will be generated. Each of these queries will be solved using GT-CFR. Eventually, the query will be a specific one that is one step from the terminal state whose values can be computed exactly and stored in  $f(\beta)$ . As this value was generated in self-play or by a query solver, and CFR is deterministic, it will produce another self-play game with the identical query, except it will load the solved value from  $f(\beta)$ , and inductively the values will get propagated from the bottom up. Since CFR is deterministic and  $T$  is finite, these ensure that the memory requirement is not infinite despite the continuous-valued keys.

Practically, the success of the training process will depend on the representational capacity and training efficacy of the function approximation (*i.e.* neural network architecture).

## 3.5 Bringing it all Together: Full Algorithm Overview

The PoG algorithm learns via sound self-play: each player, when faced with a decision to make, employs a sound growing-tree CFR search equipped with a counterfactual value-and-policy network to generate a policy, which is then used to sample an action to take. This process generates two types of training data: search queries, which are then solved separately (sometimes recursively

generating new queries), and full-game trajectories. The training process uses the data in different ways: outcomes of the games and solved queries to train the value head of the network, and policies output from search along the main line to train the policy head of the network. In practice, the self-play data generation and training happen in parallel: actors generate the self-play data (and solve queries) while trainers learn new networks and periodically update the actors.

For a fully-detailed description of the algorithm, including hyperparameter values and specific descriptions of each process described above, see Appendix B.

## 4 Evaluation

We evaluate PoG on four games: chess, Go, heads-up no-limit Texas hold’em poker, and Scotland Yard. We also evaluate PoG on a smaller benchmark poker game Leduc hold’em and a custom Scotland Yard map, where the approximation quality compared to the optimal policy can be computed exactly.

Chess and Go are well-known classic games, both seen as grand challenges of AI [17, 24] which have driven progress in artificial intelligence since its inception. The achievement of DeepBlue beating Kasparov in 1997 is widely regarded to be the first big milestone of AI. Today, computer-playing programs remain consistently super-human, and one of the strongest and most widely-used programs is Stockfish [81]. Go emerged as the favorite new challenge domain, which was particularly difficult for classical search techniques [24]. Monte Carlo tree search [18, 39, 14] emerged as the dominant search technique in Go. The best of these programs, Crazy Stone and Zen, were able to reach the level of 6 dan amateur [70]. It was not until 2016 that AlphaGo defeated the first human professional Lee Sedol in the historical 2016 match, and also defeated the top human Ke Jie in 2017.

Heads-up no-limit Texas hold’em is the most common two-player version of poker played by humans, also played by DeepStack and Libratus [55, 11]. Human-level poker has been the standard challenge domain among imperfect information games, inspiring the field of game theory itself. no-limit Texas hold’em adds the complexity of stochastic events (card draws), imperfect information (private cards), and a very large state space [35]. We use blinds of 100 and 50 chips, and stack sizes of 200 big blinds (20,000 chips).

Scotland Yard is a compelling board game of imperfect information, receiving Spiel des Jahres award in 1983 as well as being the “The most popular game ’83” by SpielBox [67]. The game is played on a map of London, where locations are connected by edges representing different modes of transportation. One player plays as “Mr. X” (the evader) and other controls detectives (pursuers). Mr. X is not visible for most of the game, but detectives get to see the mode of transportation Mr. X uses (e.g. taxi, bus, subway). In order to win, detectives need to catch Mr. X within 24 rounds. Scotland Yard is a perfect example of a game that combines search and imperfect information: agents have to search future position while correctly reasoning about the likelihood of Mr. X’s current location. Also, Scotland Yard has partially-observable *actions*, so private information is coupled with the effects of the choices in a way that is not present in Texas hold’em poker. More detailed explanation of Scotland Yard is in Appendix D.

This suite of games covers the classic challenge domains across game types (perfect information and imperfect information, some with stochastic elements and others not), as well as a new challenging imperfect information game with significantly longer sequences of actions and a fundamentally different type of uncertainty over hidden actions.

When reporting the results we use  $\text{PoG}(s, c)$  notation from Section 3.2. As a reminder,  $s$  is the total number of expansion trajectories,  $c$  is the number of expansion trajectories per regret update phase, and  $\lceil \frac{s}{c} \rceil$  is the total number of GT-CFR iterations.

### 4.1 Exploitability in Leduc Poker and Small Scotland Yard Map

We evaluate PoG in Leduc poker [74], a commonly used benchmark poker game, and Scotland Yard on a custom map. The full description of Leduc poker and map are presented in Appendix C.

**Exploitability** is a standard metric to represent empirical convergence rates: it represents the average amount a player can gain by deviating to a best response, which is zero at equilibrium. For a given joint policy in a two-player zero-sum game  $\pi = (\pi_1, \pi_2)$ ,  $\text{EXPLOITABILITY}(\pi) = (\max_{\pi'_1} u_1(\pi'_1, \pi_2) + \max_{\pi'_2} u_2(\pi_1, \pi'_2))/2$ , where  $u_i(\pi)$  is the expected utility to player  $i$  under joint policy  $\pi$ . Exploitability is a function of a specific (fixed) joint policy. However, for a search algorithm like PoG, previous searches may affect policies computed at later points within the same game, as explained in Section 2.3. Hence, we construct multiple samples of the PoG policy by choosing a random seed, running the search algorithm at every public state in a breadth-first manner such

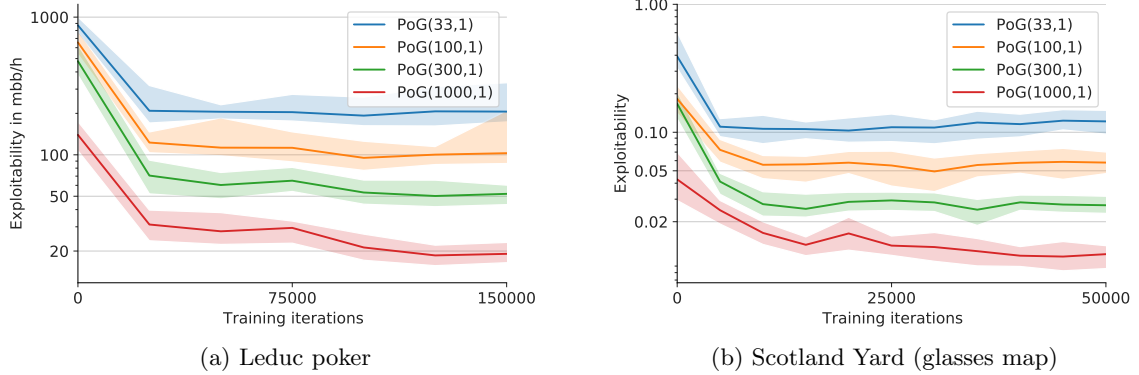


Figure 7: Exploitability of POG as a function of the number of training steps under different number of simulations of GT-CFR in (a) Leduc poker, and (b) Scotland Yard (glasses map). All networks were trained using a single training run of POG(100, 1), and the x-values correspond to a network trained for the corresponding number of steps. Each line corresponds to a different evaluation condition, *e.g.* POG( $s, c$ ) used at evaluation time. The ribbon shows minimum and maximum exploitabilities out of 50 seeded runs for each setup. The units of the y-axis in Leduc poker are milli big blinds per hand (where a milli big blind is corresponds to one thousandth of a chip in Leduc), in Scotland Yard the reward is either -1 (loss) or +1 (win).

that every search is conditioned on previous searches at predecessor states, and composing together the policies obtained from each search. We then show the minimum, average, and maximum exploitabilities over policies constructed in this way from 50 different choices of seeds. If the minimum and maximum exploitability values are tight, then they represent an accurate estimate of overall exploitability.

Figure 7 shows the convergence rates of POG in Leduc poker and the glasses map of Scotland Yard, as a function of the number of CVPN training steps. For these graphs, we evaluate multiple networks (each trained for a different number of steps) generated by a single training run of POG(100, 1). Each data point corresponds to a specific network (determined by number of steps trained) being evaluated under different settings during play. For each specific x-value, a single network was used to obtain each exploitability value of POG using the network under different evaluation conditions. We observe that exploitability drops down fairly quickly as the training steps increase. Also, even using only 1 CFR update per simulation, there is significant difference in exploitability when more simulations are used.

As Theorem 1 suggests, more training (by reducing  $\epsilon$ ) and more search (by increasing  $T$ ) reduces the exploitability of POG. Standard RL algorithms in self-play are not guaranteed to reduce exploitability with continued training in this setting. We show this lack of convergence in practice in Section C.4.

## 4.2 Results in Challenge Domains

We now present our main results: the performance of POG in chess, Go, heads-Up no-limit Texas hold’em, and Scotland Yard.

We trained a version of AlphaZero using its original settings in Chess and Go using 3500 concurrent actors using one TPUv4 each, for a total of 800k training steps. POG was trained using a similar amount of concurrent resources.

In chess, we evaluated POG against Stockfish 8, level 20 [81] and AlphaZero. POG(800, 1) was run in training for 3M training steps. During evaluation, Stockfish uses various search controls: number of threads, and time per search. We evaluate AlphaZero and POG up to 60000 simulations. A tournament between all of the agents was played at 200 games per pair of agents (100 games as white, 100 games as black). Table 1a shows the relative Elo comparison obtained by this tournament, where a baseline of 0 is chosen for Stockfish(threads=1, time=0.1s).

In Go, we evaluate POG(60000, 10) using a similar tournament as in Chess, against two previous Go programs: GnuGo (at its highest level, 10) [80] and Pachi v7.0.0 [5] with 10k and 100k simulations, as well as AlphaZero [71]. The POG network was trained for 1M training steps. Table 1b shows the relative Elo comparison for a subset of the agents that played in this tournament, where a baseline of 0 is chosen for GnuGo. The full results are presented in Appendix C.

Agent	Rel. Elo
AlphaZero(sims=60k)	+592
Stockfish(threads=16, time=4s)	+530
AlphaZero(sims=8k)	+455
<b>PoG(s=60k, c=10)</b>	<b>+420</b>
Stockfish(threads=4, time=1s)	+382
<b>PoG(s=8k, c=10)</b>	<b>+268</b>
Stockfish(threads=1, time=0.1s)	0

(a) Chess results. Elo of Stockfish with a single thread and 100ms thinking time was set to be 0. The other values are relative to that.

Table 1: A table with relative Elo of different agents. Each agent played 200 matches (100 as white and 100 as black) against every other agent in the tournament.

Agent	Rel. Elo
AlphaZero(s=16k, t=800k)	+3139
AlphaZero(s=8k, t=800k)	+2875
<b>PoG(s=16k, c=10)</b>	<b>+1970</b>
<b>PoG(s=8k, c=10)</b>	<b>+1902</b>
Pachi(s=100k)	+869
Pachi(s=10k)	+231
GnuGo(l=10)	0

(b) Go results. Elo of GnuGo was set to be 0. AlphaZero(s=16k, t=800k) refers to 16000 search simulations. For full results, see Appendix C.

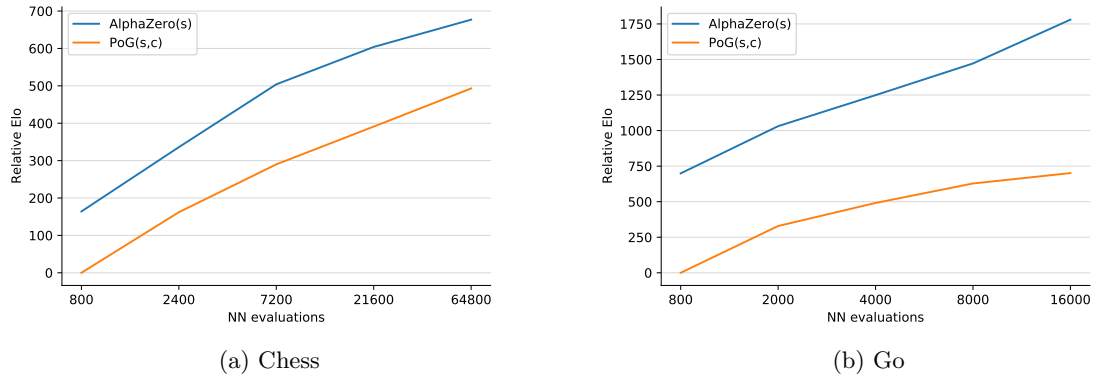


Figure 8: Scalability of PoG with increasing number of neural network evaluations compared to AlphaZero measured on relative Elo scale. The x-axis corresponds to the number of simulations in AlphaZero and  $s$  in  $\text{PoG}(s, c)$ .

For chess and Go, we also present direct Elo comparisons when increasing the number of neural network evaluations in Figure 8. Note that while the neural networks evaluations account for the majority of the run time, the complexity of the regret update phase is linear in the size of the tree. The run time is thus quadratic in the number of GT-CFR iterations. The absolute time cost could be reduced by an implementation that runs the regret update and expansion phase in parallel. For a more detailed analysis of PoG’s complexity, see Section B.2.

We notice in both chess and Go that PoG reaches strong performance. In Chess, PoG(60000,10) is stronger than Stockfish using 4 threads and one second of search time. In Go, PoG(16000, 10) is more than 1100 Elo stronger than Pachi with 100,000 simulations. Also, PoG(16000, 10) wins 0.5% (2/400) of its games against the strongest AlphaZero( $s=8000, t=800k$ ). As a result, PoG appears to be performing at the level of top human amateur, possibly even professional level. In both cases, PoG is weaker than AlphaZero, with the gap being smaller in Chess. We hypothesize that this difference is the result of MCTS being more efficient than CFR on perfect information games, as the price of PoG’s generality.

In heads-up no-limit Texas hold’em, we evaluate PoG against Slumbot2019 [34, 33], the best openly-available computer poker player. When training poker, PoG uses randomized betting abstractions described in Section B.7 to reduce the number of actions from 20,000 to 4 or 5. PoG(10,0.1) is trained for up to 1.1M training steps and then evaluated. Since poker has particularly high variance, we use AIVAT [16] to compute a more accurate estimate of performance. Head-to-head results are shown in Table 9. PoG(10,0.01) wins on average  $7 \pm 3$  milli big blinds (0.7 chips) per hand, with 95% confidence intervals (3.1M matches). We also evaluate PoG against a local best-response (LBR) player that can use only fold and call actions with a poker-specific heuristic which has shown to find exploits in previous poker agents [47]. LBR fails to find an exploit of PoG’s strategy, and PoG wins on average by  $434 \pm 9$  milli big blinds per hand. Table 9 summarizes the results of PoG along with other recent poker agents.

Agent Name	Slumbot	LBK [47]
Slumbot (2016)	-	-522 $\pm$ 50
ARMAC [26]	-	-460 $\pm$ 260
DeepStack [55]	-	428 $\pm$ 87
Modicum [13]	11 $\pm$ 5	-
ReBeL [7]	45 $\pm$ 5	-
Supremus [85]	176 $\pm$ 44	951 $\pm$ 96
POG(10, 0.01)	7 $\pm$ 3	434 $\pm$ 9

Figure 9: Head-to-head results showing expected winnings of PoG (mbb/h) against Slumbot and LBR together with results of other recently published agents. The LBR agent use either fold or call (FC) actions in the all four rounds. The  $\pm$  shows one standard deviation. LBR results for Slumbot are from [47]. The other results are from the papers describing the agents.

In Scotland Yard, the current state-of-the-art agent in this game is based on MCTS with game-specific heuristic enhancements [59]. We call this agent ‘‘PimBot’’ based on its main author, Joseph Antonius Maria (‘‘Pim’’) Nijssen. PimBot implements a variant of MCTS that uses determinization and heuristic evaluations and playout policies [59, 58]. PimBot won 34 out of 50 manually played games against the Nintendo DS Scotland Yard AI.

In our experiment POG is trained up to 17M steps. In evaluation we play a head-to-head match with PoG(400, 1) against PimBot at different number of simulations per search. The results are shown in Figure 10. These results show that PoG is winning significantly even against PimBot with 10M search simulations (55% win rate), compared to PoG searching a tiny fraction of the game. Interestingly PimBot doesn’t seem to play stronger with more search at this point, as both the 1M and 10M iteration versions have the same performance against PoG.

As in chess and Go, PoG also demonstrates strong performance in these complex imperfect information games. In the case of poker, in addition to beating Slumbot it also beats the local best-response agent which was not possible for some previous agents (including Slumbot). Finally, PoG significantly beats the state-of-the-art agent in Scotland Yard, an imperfect information game with longer episodes and fundamentally different kind of imperfect information than in poker. Together, these results indicate that PoG is capable of strong performance across four games, two fundamentally different game types, and can act as a truly unified algorithm combining search, learning, and game-theoretic reasoning for competitive games.

## 5 Related Work

Player of Games builds upon several components that have been developed in previous work. In this section, we describe the most relevant of these past works and how they relate to PoG.

PoG combines many elements that were originally proposed in AlphaZero and its predecessors, as well as DeepStack [70, 72, 71, 55]. Specifically, PoG uses the combined search and learning using deep neural networks from AlphaGo and DeepStack, along with game-theoretic reasoning and search in imperfect information games from DeepStack. The use of public belief states and decomposition in imperfect information games has been a critical component of success in no-limit Texas Hold’em poker [15, 10, 55, 11, 13, 12, 7]. The main difference from AlphaZero is that the search and self-play training in PoG are also sound for imperfect information games, and evaluation across game types. The main difference from DeepStack is the use of significantly less domain knowledge: the use of self-play (rather than poker-specific heuristics) to generate training data and a single network for all stages of the game. The most closely related algorithm is Recurrent Belief-based Learning (ReBeL) [7]. Like PoG, ReBeL combines search, learning, and game-theoretic reasoning via self-play. The main difference is that PoG is based on (safe) continual resolving and sound self-play. To achieve ReBeL’s guarantees, its test-time search must be conducted with the same algorithm as in training, whereas PoG can use any belief-based value-and-policy network of the form described in Section 3.1 (similarly to e.g. AlphaZero, which trains using 800 simulations but then can use substantially larger simulation limits at test-time). PoG is also validated empirically across many

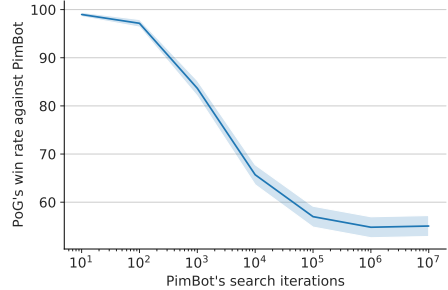


Figure 10: Win rate of PoG(400, 1) against PimBot with varying simulations. 2000 matches were played for each data point, with roles swapped for half of the matches. Note that the x-axis has logarithmic scale. The ribbon shows 95% confidence interval.

different challenge games of different game types.

There has been considerable work in search for imperfect information games. One method that has been quite successful in practice is determinization: at decision-time, a set of candidate world states are sampled, and some form of search is performed [19, 51]. In fact, PimBot [59, 58] is based on these methods and achieved state-of-the art results in Scotland Yard. However, these methods are not guaranteed to converge to an optimal strategy over time. We demonstrate this lack of convergence in practice over common search algorithms and standard RL benchmarks in Section C.4. In contrast, the search in POG is based on game-theoretic reasoning. Other algorithms have proposed adding game-theoretic reasoning to search: Smooth UCT [28] combines UCT [39] with fictitious play, however its convergence properties are not known. Online Outcome Sampling [48] derives an MCTS variant of Monte Carlo CFR [42]; however, OOS is only guaranteed to approach an approximate equilibrium at a single information state (local consistency) and has not been evaluated in large games. GT-CFR used by POG makes use of sound search based on decomposition and is globally consistent [15, 84].

There have been a number of RL algorithms that have been proposed for two-player zero-sum games: Fictitious Self-Play [29, 30], Policy-Space Response Oracles (PSRO) [43, 56, 54], Double Neural CFR [46], Deep CFR and DREAM [8, 76], Regret Policy Gradients [75], Exploitability Descent [50], Neural Replicator Dynamics (NeuRD) [31], Advantage Regret-Matching Actor Critic [26], Friction FoReL [60], MAIO [57], Extensive-form Double Oracle (XDO) [53], and Neural Auto-curricula (NAC) [21]. These methods adapt classical algorithms for computing (approximate) Nash equilibria to the RL setting with sampled experience and general function approximation. As such, they combine game-theoretic reasoning and learning. Several of these methods have shown promise to scale: Pipeline PSRO defeated the best openly available agent in Stratego Barrage; Deep CFR, DREAM, and ARMAC showed promising results on large poker games. Combined with human data, AlphaStar was able to use game-theoretic reasoning to create master-level real-time strategy policy [83]. However, none of them can use search at test-time to refine their policy.

Lastly, there have been works that use some combination of search, learning, and/or game-theoretic reasoning applied to specific domains. Neural networks have been trained via Q-learning to learn to play Scotland Yard [20]; however, the overall play strength of the resulting policy was not directly compared to any other known Scotland Yard agent. In poker, Supremus proposed a number of improvements to DeepStack and demonstrated that they make a big difference when playing human experts [85]. Another work used a method inspired by DeepStack applied to The Resistance [69]. In the cooperative setting, several works have made use of belief-based learning (and search) using public subgame decomposition [22, 45, 73], applied to Hanabi [4]. Search and reinforcement learning were combined to produce a bridge bidding player that cooperated with a state-of-the-art bot (WBridge5) and with humans [49]. Learning and game-theoretic reasoning were also recently combined to produce agents that play well with humans without human data on the collaborative game Overcooked [77]. Of considerable note is the game of (no-press) Diplomacy. Game-theoretic reasoning was combined with learning in Best Response Policy Iteration [2]. Game-theoretic search and supervised learning were employed in [25] reaching human-level performance on the two-player variant. Recently, all three were combined in DORA [3] which learned to play Diplomacy without human data, and also reached human-level performance on the two-player variant. The main difference between POG and these works is that they focus on specific games and exploit domain-specific knowledge to attain strong performance.

## 6 Conclusion

In this paper, we describe Player of Games (POG) a unified algorithm that combines search, learning, and game-theoretic reasoning. POG is comprised of two main components: a novel growing-tree counterfactual regret minimization (GT-CFR), and sound self-play whichs learn counterfactual value-and-policy networks via self-play. Most notably, POG is a sound algorithm for both perfect *and* imperfect information games: as computational resources increase, POG is guaranteed to produce better approximation of minimax-optimal strategies. This finding is also verified empirically in Leduc poker, where additional search leads to test-time approximation refinement, unlike any pure reinforcement learning algorithms that do not use search.

POG is the first sound algorithm in this class to demonstrate strong performance on challenge domains, using minimal domain knowledge. In the perfect information games of chess and Go, POG performs at the level of human experts or professionals, but can be significantly weaker than specialized algorithms for this class of games, like AlphaZero, when given the same resources. In

the imperfect information game no-limit Texas hold’em poker, PoG beats Slumbot, the best openly available poker agent, and is shown not to be exploited by a local best-response agent using poker-specific heuristics. In Scotland Yard, PoG defeats the state-of-the-art agent.

There are some limitations of PoG that are worth investigating in future work. First, the use of betting abstractions in poker could be removed in favor of a general action-reduction policy for large action spaces. Second, PoG currently requires enumerating the information states per public state which can be prohibitively expensive in some games; this might be approximated by a generative model that samples world states and operates on the sampled subset. Finally, significant computational resources are used to attain strong play in challenge domains; an interesting question is whether this level of play is achievable with less computational resources.

## 7 Acknowledgments

We would like to thank several people for their help and feedback: Ed Lockhart, Michael Johanson, Adam White, Julian Schrittwieser, Thomas Hubert, Michal Sustr, Leslie Acker, Morgan Redshaw, Dustin Morrill, Trevor Davis, Stephen McAleer, and Sanah Choudry.

We would like to extend a special thanks to Mark Winands and Pim Nijssen for providing the code for and helping us configure their Scotland Yard agent, and special thanks to Eric Jackson for providing the code for and assistance with his poker agent.

## References

- [1] Martín Abadi, Paul Barham, Jianmin Chen, Zhifeng Chen, Andy Davis, Jeffrey Dean, Matthieu Devin, Sanjay Ghemawat, Geoffrey Irving, Michael Isard, et al. Tensorflow: A system for large-scale machine learning. In *12th USENIX symposium on operating systems design and implementation (OSDI 16)*, pages 265–283, 2016.
- [2] Thomas W. Anthony, Tom Eccles, Andrea Tacchetti, János Kramár, Ian M. Gemp, Thomas C. Hudson, Nicolas Porcel, Marc Lanctot, Julien Pérolat, Richard Everett, Satinder Singh, Thore Graepel, and Yoram Bachrach. Learning to play no-press Diplomacy with best response policy iteration. In *Thirty-third Conference on Neural Information Processing Systems (NeurIPS)*, 2020.
- [3] Anton Bakhtin, David Wu, Adam Lerer, and Noam Brown. No-press Diplomacy from scratch. In *Proceedings of the Thirty-fourth Conference on Neural Information Processing Systems (NeurIPS)*, 2021.
- [4] Nolan Bard, Jakob N. Foerster, Sarath Chandar, Neil Burch, Marc Lanctot, H. Francis Song, Emilio Parisotto, Vincent Dumoulin, Subhodeep Moitra, Edward Hughes, Iain Dunning, Shibley Mourad, Hugo Larochelle, Marc G. Bellemare, and Michael Bowling. The Hanabi challenge: A new frontier for ai research. *Artificial Intelligence*, 280, 2020.
- [5] Petr Baudis, Jean loup Gailly, and Lemonsqueeze. Pachi: Software for the board game of go / weiqi / baduk, 2016. <https://pachi.or.cz/>.
- [6] Michael Bowling, Neil Burch, Michael Johanson, and Oskari Tammelin. Heads-up limit Hold’em poker is solved. *Science*, 347(6218):145–149, January 2015.
- [7] Noam Brown, Anton Bakhtin, Adam Lerer, and Qucheng Gong. Combining deep reinforcement learning and search for imperfect-information games. In *Thirty-fourth Annual Conference on Neural Information Processing Systems (NeurIPS)*, 2020. <https://arxiv.org/abs/2007.13544>.
- [8] Noam Brown, Adam Lerer, Sam Gross, and Tuomas Sandholm. Deep counterfactual regret minimization. *CoRR*, abs/1811.00164, 2018.
- [9] Noam Brown and Tuomas Sandholm. Strategy-based warm starting for regret minimization in games. In *Proceedings of the AAAI Conference on Artificial Intelligence*, volume 30, 2016.
- [10] Noam Brown and Tuomas Sandholm. Safe and nested subgame solving for imperfect-information games. In *Proceedings of the 31st Conference on Neural Information Processing Systems (NIPS)*, 2017.

- [11] Noam Brown and Tuomas Sandholm. Superhuman AI for heads-up no-limit poker: Libratus beats top professionals. *Science*, 360(6385), December 2017.
- [12] Noam Brown and Tuomas Sandholm. Superhuman AI for multiplayer poker. *Science*, 365(6456):885–890, 2019.
- [13] Noam Brown, Tuomas Sandholm, and Brandon Amos. Depth-limited solving for imperfect-information games. In *Proceedings of the Thirty-second Conference on Neural Information Processing Systems*, 2018.
- [14] Cameron B. Browne, Edward Powley, Daniel Whitehouse, Simon M. Lucas, Peter I. Cowling, Philipp Rohlfshagen, Stephen Tavener, Diego Perez, Spyridon Samothrakis, and Simon Colton. A survey of monte carlo tree search methods. *IEEE Transactions on Computational Intelligence and AI in Games*, 4(1):1–43, 2012.
- [15] Neil Burch, Michael Johanson, and Michael Bowling. Solving imperfect information games using decomposition. In *Proceedings of the Twenty-Eighth AAAI Conference on Artificial Intelligence (AAAI)*, 2014.
- [16] Neil Burch, Martin Schmid, Matej Moravčík, and Michael Bowling. AIVAT: A new variance reduction technique for agent evaluation in imperfect information games, 2017.
- [17] Murray Campbell, A. Joseph Hoane, and Feng-hsiung Hsu. Deep blue. *Artificial Intelligence*, 134(1–2):57–83, January 2002.
- [18] Rémi Coulom. Efficient selectivity and backup operators in Monte-Carlo tree search. In H. Jaap van den Herik, Paolo Ciancarini, and H. H. L. M. (Jeroen) Donkers, editors, *Computers and Games*, pages 72–83, Berlin, Heidelberg, 2007. Springer Berlin Heidelberg.
- [19] Peter I. Cowling, Edward J. Powley, and Daniel Whitehouse. Information set Monte Carlo tree search. *IEEE Transactions on Computational Intelligence and AI in Games*, 4:120–143.
- [20] Tirtharaj Dash, Sahith N Dambekodi, Preetham N Reddy, and Ajith Abraham. Adversarial neural networks for playing hide-and-search board game Scotland Yard. *Neural Computing and Applications*, 32(8):3149–3164, 2018.
- [21] Xidong Feng, Oliver Slumbers, Ziyu Wan, Bo Liu, Stephen Marcus McAleer, Ying Wen, Jun Wang, and Yaodong Yang. Neural auto-curricula in two-player zero-sum games. In *Proceedings of the Thirty-fifth Conference on Neural Information Processing Systems (NeurIPS)*, 2021.
- [22] Jakob N. Foerster, Francis Song, Edward Hughes, Neil Burch, Iain Dunning, Shimon Whiteson, Matthew Botvinick, and Michael Bowling. Bayesian action decoder for deep multi-agent reinforcement learning, 2019.
- [23] Kunihiko Fukushima. Neocognitron: A self-organizing neural network model for a mechanism of pattern recognition unaffected by shift in position. *Biological Cybernetics*, 36:193–202, 1980.
- [24] Sylvain Gelly, Levente Kocsis, Marc Schoenauer, Michèle Sebag, David Silver, Csaba Szepesvári, and Olivier Teytaud. The grand challenge of computer Go: Monte Carlo tree search and extensions. *Communications of the ACM*, 55(3):106–113, March 2012.
- [25] Jonathan Gray, Adam Lerer, Anton Bakhtin, and Noam Brown. Human-level performance in no-press Diplomacy via equilibrium search. In *In Proceedings of the International Conference on Learning Representations (ICLR)*, 2020.
- [26] Audriūnas Gruslys, Marc Lanctot, Rémi Munos, Finbarr Timbers, Martin Schmid, Julien Perolat, Dustin Morrill, Vinicius Zambaldi, Jean-Baptiste Lespiau, John Schultz, Mohammad Gheshlaghi Azar, Michael Bowling, and Karl Tuyls. The advantage regret-matching actor-critic, 2020.
- [27] S. Hart and A. Mas-Colell. A simple adaptive procedure leading to correlated equilibrium. *Econometrica*, 68(5):1127–1150, 2000.
- [28] J. Heinrich and D. Silver. Smooth UCT search in computer poker. In *Proceedings of the 24th International Joint Conference on Artificial Intelligence (IJCAI)*, 2015.

[29] Johannes Heinrich, Marc Lanctot, and David Silver. Fictitious self-play in extensive-form games. In *Proceedings of the 32nd International Conference on Machine Learning (ICML 2015)*, 2015.

[30] Johannes Heinrich and David Silver. Deep reinforcement learning from self-play in imperfect-information games. *CoRR*, abs/1603.01121, 2016.

[31] Daniel Hennes, Dustin Morrill, Shayegan Omidshafiei, Remi Munos, Julien Perolat, Marc Lanctot, Audrunas Gruslys, Jean-Baptiste Lespiau, Paavo Parmas, Edgar Duenez-Guzman, and Karl Tuyls. Neural replicator dynamics. In *Proceedings of the International Conference on Autonomous Agents and Multiagent Systems (AAMAS)*, 2020.

[32] Peter J. Huber. Robust Estimation of a Location Parameter. *The Annals of Mathematical Statistics*, 35(1):73 – 101, 1964.

[33] Eric Jackson. Slumbot github repository. <https://github.com/ericgjackson/slumbot2017>.

[34] Eric Jackson. Slumbot NL: Solving large games with counterfactual regret minimization using sampling and distributed processing. In *Proceedings of the Computer Poker and Imperfect Information: Papers from the AAAI 2013 Workshop*, 2013. <https://github.com/ericgjackson/slumbot2019>.

[35] Michael Johanson. Measuring the size of large no-limit poker games, 2013.

[36] Michael Johanson, Nolan Bard, Marc Lanctot, Richard Gibson, and Michael Bowling. Efficient nash equilibrium approximation through Monte Carlo counterfactual regret minimization. In *Proceedings of the Eleventh International Conference on Autonomous Agents and Multi-Agent Systems (AAMAS)*, 2012.

[37] Michael Bradley Johanson. *Robust Strategies and Counter-Strategies: From Superhuman to Optimal Play*. PhD thesis, University of Alberta, 2016. <http://johanson.ca/publications/theses/2016-johanson-phd-thesis/2016-johanson-phd-thesis.pdf>.

[38] Donald E. Knuth and Ronald W. Moore. An analysis of alpha-beta pruning. *Artificial Intelligence*, 6(4):293–326, 1975.

[39] Levente Kocsis and Csaba Szepesvári. Bandit based Monte-Carlo planning. In *In: ECML-06. Number 4212 in LNCS*, pages 282–293. Springer, 2006.

[40] Vojtech Kovářík, Martin Schmid, Neil Burch, Michael Bowling, and Viliam Lisý. Rethinking formal models of partially observable multiagent decision making. *AIJ*, to appear, 2021.

[41] Marc Lanctot, Edward Lockhart, Jean-Baptiste Lespiau, Vinicius Zambaldi, Satyaki Upadhyay, Julien Perolat, Sriram Srinivasan, Finbarr Timbers, Karl Tuyls, Shayegan Omidshafiei, Daniel Hennes, Dustin Morrill, Paul Muller, Timo Ewalds, Ryan Faulkner, János Kramár, Bart De Vylder, Brennan Saeta, James Bradbury, David Ding, Sebastian Borgeaud, Matthew Lai, Julian Schrittwieser, Thomas Anthony, Edward Hughes, Ivo Danihelka, and Jonah Ryan-Davis. OpenSpiel: A framework for reinforcement learning in games. *CoRR*, abs/1908.09453, 2019.

[42] Marc Lanctot, Kevin Waugh, Martin Zinkevich, and Michael Bowling. Monte Carlo sampling for regret minimization in extensive games. In *Advances in Neural Information Processing Systems 22 (NIPS)*, pages 1078–1086, 2009.

[43] Marc Lanctot, Vinicius Zambaldi, Audrunas Gruslys, Angeliki Lazaridou, Karl Tuyls, Julien Perolat, David Silver, and Thore Graepel. A unified game-theoretic approach to multiagent reinforcement learning. In *Advances in Neural Information Processing Systems*, 2017.

[44] Adam Lerer, Hengyuan Hu, Jakob Foerster, and Noam Brown. Improving policies via search in cooperative partially observable games. In *Proceedings of the AAAI Conference on Artificial Intelligence*, 2020.

[45] Adam Lerer, Hengyuan Hu, Jakob Foerster, and Noam Brown. Improving policies via search in cooperative partially observable games. In *Proceedings of the Thirty-Fourth AAAI Conference on Artificial Intelligence*, 2020.

[46] Hui Li, Kailiang Hu, Shaohua Zhang, Yuan Qi, and Le Song. Double neural counterfactual regret minimization. In *Proceedings of the Eighth International Conference on Learning Representations (ICLR)*, 2019.

[47] Viliam Lisý and Michael Bowling. Eqilibrium approximation quality of current no-limit poker bots. In *Workshops at the Thirty-First AAAI Conference on Artificial Intelligence*, 2017.

[48] Viliam Lisý, Marc Lanctot, and Michael Bowling. Online Monte Carlo counterfactual regret minimization for search in imperfect information games. In *Proceedings of the Fourteenth International Conference on Autonomous Agents and Multi-Agent Systems (AAMAS)*, pages 27–36, 2015.

[49] Edward Lockhart, Neil Burch, Nolan Bard, Sébastien Borgeaud, Tom Eccles, Lucas Smaira, and Ray Smith. Human-agent cooperation in bridge bidding. In *Proceedings of the Cooperative AI Workshop at 34th Conference on Neural Information Processing Systems (NeurIPS 2020)*, 2020.

[50] Edward Lockhart, Marc Lanctot, Julien Pérolat, Jean-Baptiste Lespiau, Dustin Morrill, Finbarr Timbers, and Karl Tuyls. Computing approximate equilibria in sequential adversarial games by exploitability descent. In *Proceedings of the 28th International Joint Conference on Artificial Intelligence (IJCAI)*, 2019.

[51] Jeffrey Long, Nathan R. Sturtevant, Michael Buro, and Timothy Furtak. Understanding the success of perfect information Monte Carlo sampling in game tree search. In *Proceedings of the Twenty-Fourth AAAI Conference on Artificial Intelligence*, AAAI’10, page 134–140. AAAI Press, 2010.

[52] T. A. Marsland and M. Campbell. A survey of enhancements to the alpha-beta algorithm. In *Proceedings of the ACM ’81 Conference*, ACM ’81, page 109–114, New York, NY, USA, 1981. Association for Computing Machinery.

[53] Stephen McAleer, John Lanier, Pierre Baldi, and Roy Fox. Xdo: A double oracle algorithm for extensive-form games. In *Proceedings of the Thirty-fifth Conference on Neural Information Processing Systems (NeurIPS)*, 2021.

[54] Stephen McAleer, John Lanier, Roy Fox, and Pierre Baldi. Pipeline PSRO: A scalable approach for finding approximate nash equilibria in large games. In *Proceedings of the Thirty-fourth Conference on Neural Information Processing Systems (NeurIPS)*, 2020.

[55] Matej Moravčík, Martin Schmid, Neil Burch, Viliam Lisý, Dustin Morrill, Nolan Bard, Trevor Davis, Kevin Waugh, Michael Johanson, and Michael Bowling. Deepstack: Expert-level artificial intelligence in heads-up no-limit poker. *Science*, 358(6362), October 2017.

[56] Paul Muller, Shayegan Omidshafiei, Mark Rowland, Karl Tuyls, Julien Perolat, Siqi Liu, Daniel Hennes, Luke Marris, Marc Lanctot, Edward Hughes, Zhe Wang, Guy Lever, Nicolas Heess, Thore Graepel, and Remi Munos. A generalized training approach for multiagent learning. In *Proceedings of the Eighth International Conference on Learning Representations (ICLR)*, 2020.

[57] Remi Munos, Julien Perolat, Jean-Baptiste Lespiau, Mark Rowland, Bart De Vylder, Marc Lanctot, Finbarr Timbers, Daniel Hennes, Shayegan Omidshafiei, Audrunas Gruslys, Mohammad Gheshlaghi Azar, Edward Lockhart, and Karl Tuyls. Fast computation of Nash equilibria in imperfect information games. In *Proceedings of the International Conference on Machine Learning (ICML)*, 2020.

[58] J.A.M. Nijssen. *Monte-Carlo Tree Search for Multi-Player Games*. PhD thesis, Maastricht University, 2013.

[59] J.A.M. Nijssen and M.H.M. Winands. Monte-Carlo tree search for the hide-and-seek game scotland yard. *IEEE Transactions on Computational Intelligence and AI in Games*, 4(4):282–294, 2012.

[60] Julien Perolat, Remi Munos, Jean-Baptiste Lespiau, Shayegan Omidshafiei, Mark Rowland, Pedro Ortega, Neil Burch, Thomas Anthony, David Balduzzi, Bart De Vylder, Georgios Piliouras, Marc Lanctot, and Karl Tuyls. From Poincaré recurrence to convergence in imperfect information games: Finding equilibrium via regularization. In *Proceedings of the The Thirty-eighth International Conference on Machine Learning (ICML)*, 2021.

[61] Stuart J. Russell and Peter Norvig. *Artificial Intelligence: A Modern Approach*. Pearson Education, 2nd edition, 2003.

[62] Arthur L. Samuel. Some studies in machine learning using the game of checkers. *IBM Journal of Research and Development*, 44:206–226, 1959.

[63] Jonathan Schaeffer and Aske Plaat. New advances in alpha-beta searching. In *CSC '96*, 1996.

[64] Martin Schmid. *Search in Imperfect Information Games*. PhD thesis, 2021. Also available at <https://arxiv.org/abs/2111.05884>.

[65] Martin Schmid, Neil Burch, Marc Lanctot, Matej Moravcik, Rudolf Kadlec, and Michael Bowling. Variance reduction in Monte Carlo counterfactual regret minimization (VR-MCCFR) for extensive form games using baselines. In *Proceedings of the The Thirty-Third AAAI Conference on Artificial Intelligence*, 2019.

[66] Martin Schmid, Matej Moravcik, and Milan Hladik. Bounding the support size in extensive form games with imperfect information. In *Twenty-Eighth AAAI Conference on Artificial Intelligence*, 2014.

[67] Game of the year 1983: Scotland Yard. <https://www.spiel-des-jahres.de/spiel-des-jahres-1983-scotland-yard/>. Accessed: 2020-Jan-30.

[68] Richard B. Segal. On the scalability of parallel UCT. In *CG'10: Proceedings of the 7th international conference on Computers and games*, pages 36–47, 2010.

[69] Jack Serrino, Max Kleiman-Weiner, David C. Parkes, and Joshua B. Tenenbaum. Finding friend and foe in multi-agent games. In *Proceedings of the Thirty-third Conference on Neural Information Processing Systems (NeurIPS)*, 2019.

[70] David Silver, Aja Huang, Chris J. Maddison, Arthur Guez, Laurent Sifre, George van den Driessche, Julian Schrittwieser, Ioannis Antonoglou, Veda Panneershelvam, Marc Lanctot, Sander Dieleman, Dominik Grewe, John Nham, Nal Kalchbrenner, Ilya Sutskever, Timothy Lillicrap, Madeleine Leach, Koray Kavukcuoglu, Thore Graepel, and Demis Hassabis. Mastering the game of Go with deep neural networks and tree search. *Nature*, 529:484–489, 2016.

[71] David Silver, Thomas Hubert, Julian Schrittwieser, Ioannis Antonoglou, Matthew Lai, Arthur Guez, Marc Lanctot, Laurent Sifre, Dharshan Kumaran, Thore Graepel, Timothy Lillicrap, Karen Simonyan, and Demis Hassabis. A general reinforcement learning algorithm that masters chess, shogi, and Go through self-play. *Science*, 632(6419):1140–1144, 2018.

[72] David Silver, Julian Schrittwieser, Karen Simonyan, Ioannis Antonoglou, Aja Huang, Arthur Guez, Thomas Hubert, Lucas Baker, Matthew Lai, Adrian Bolton, Yutian Chen, Timothy Lillicrap, Fan Hui, Laurent Sifre, George van den Driessche, Thore Graepel, and Demis Hassabis. Mastering the game of Go without human knowledge. *Nature*, 550(7676):354–359, 2017.

[73] Samuel Sokota, Edward Lockhart, Finbarr Timbers, Elnaz Davoodi, Ryan D’Orazio, Neil Burch, Martin Schmid, Michael Bowling, and Marc Lanctot. Solving common-payoff games with approximate policy iteration. In *Proceedings of the Thirty-Fifth AAAI Conference on Artificial Intelligence*, 2021.

[74] Finnegan Southey, Michael Bowling, Bryce Larson, Carmelo Piccione, Neil Burch, Darse Billings, and Chris Rayner. Bayes’ bluff: Opponent modelling in poker. In *Proceedings of the Twenty-First Conference on Uncertainty in Artificial Intelligence (UAI)*, pages 550–558, 2005.

[75] Sriram Srinivasan, Marc Lanctot, Vinicius Zambaldi, Julien Pérolat, Karl Tuyls, Rémi Munos, and Michael Bowling. Actor-critic policy optimization in partially observable multiagent environments. In *Advances in Neural Information Processing Systems (NeurIPS)*, 2018.

[76] Eric Steinberger, Adam Lerer, and Noam Brown. DREAM: Deep regret minimization with advantage baselines and model-free learning, 2020.

[77] DJ Strouse, Kevin R. McKee, Matt Botvinick, Edward Hughes, and Richard Everett. Collaborating with humans without human data. In *Proceedings of the Thirty-fifth Conference on Neural Information Processing Systems*, 2021.

[78] Michal Šustr, Vojtěch Kovařík, and Viliam Lisý. Monte Carlo continual resolving for online strategy computation in imperfect information games. In *Proceedings of the 18th International Conference on Autonomous Agents and MultiAgent Systems*, pages 224–232, 2019.

- [79] Oskari Tammelin, Neil Burch, Michael Johanson, and Michael Bowling. Solving heads-up limit Texas Hold’em. In *Proceedings of the 24th International Joint Conference on Artificial Intelligence*, 2015.
- [80] The GnuGo Development Team. GnuGo, 2009. <https://www.gnu.org/software/gnugo/>.
- [81] The Stockfish Development Team. Stockfish: Open source chess engine, 2021. <https://stockfishchess.org/>.
- [82] Gerald Tesauro. TD-Gammon, a self-teaching backgammon program, achieves master-level play. *Neural Comput.*, 6(2):215–219, March 1994.
- [83] Oriol Vinyals, Igor Babuschkin, Wojciech M. Czarnecki, Michaël Mathieu, Andrew Dudzik, Junyoung Chung, David H. Choi, Richard Powell, Timo Ewalds, Petko Georgiev, Junhyuk Oh, Dan Horgan, Manuel Kroiss, Ivo Danihelka, Aja Huang, Laurent Sifre, Trevor Cai, John P. Agapiou, Max Jaderberg, Alexander S. Vezhnevets, Rémi Leblond, Tobias Pohlen, Valentin Dalibard, David Budden, Yury Sulsky, James Molloy, Tom L. Paine, Caglar Gulcehre, Ziyu Wang, Tobias Pfaff, Yuhuai Wu, Roman Ring, Dani Yogatama, Dario Wünsch, Katrina McKinney, Oliver Smith, Tom Schaul, Timothy Lillicrap, Koray Kavukcuoglu, Demis Hassabis, Chris Apps, and David Silver. Grandmaster level in StarCraft II using multi-agent reinforcement learning. *Nature*, 575(7782):350–354, 2019.
- [84] Michal Šustr, Martin Schmid, Matej Moravčík, Neil Burch, Marc Lanctot, and Michael Bowling. Sound search in imperfect information games. In *Proceedings of the International Conference on Autonomous Agents and Multiagent Systems (AAMAS)*, 2020.
- [85] Ryan Zarick, Bryan Pellegrino, Noam Brown, and Caleb Banister. Unlocking the potential of deep counterfactual value networks. *CoRR*, abs/2007.10442, 2020.
- [86] Martin Zinkevich, Michael Johanson, Michael Bowling, and Carmelo Piccione. Regret minimization in games with incomplete information. In *Advances in Neural Information Processing Systems 20 (NIPS)*, pages 905–912, 2008.

## A An example of Factored-Observation Stochastic Game

Figure 11 uses the notation introduced in Sec. 2 to show an example of simple FOSG game that illustrates how the histories, information states and observations interact. Follow-up Figure 12 shows a view of a game through public tree perspective.

## B Player of Games Algorithm Details

### B.1 Re-solving Process

Recall that the re-solving step and the corresponding auxiliary game requires i) the current player’s ranges ii) the opponent’s counterfactual values. This provides succinct and sufficient representation to safely re-solve the subgame rooted in a public state  $s_{pub}$ . DeepStack and Libratus then simply retrieved these invariants from its last search tree (i.e. the search tree from when it acted previously). This was possible because the search tree was fixed to a particular domain (Texas hold’em poker), and thus guaranteed that it included invariants for any possible state the agent could act in next.

As the Player of Games is a general algorithm, it can no longer leverage this special case. The current public state  $s_{pub}$  might not have been included in the last search tree, and the prior computation does not directly provide us with the required invariants for re-solving the subgame rooted in  $s_{pub}$ . POG thus starts its re-solving process in the state closest to the current state that is included in the last search tree:  $s_{pub}^{last}$ . To make sure the search procedure produces policy for the current state, we initialize the search tree to a path from  $s_{pub}^{last}$  to  $s_{current}^{last}$ . See also Figure 13.

To focus the computation on the states relevant for the current decision, the search tree is being expanded from the current public state  $s_{current}$ . Concretely, recall that the Player of Games algorithm consists of two distinct phases i) the regret update phase and ii) expansion trajectories. The regret update phase is always being run on the full tree (starting in the  $s_{current}^{last}$ ). The expansion simulations then start from  $s_{current}^{pub}$ .

Of course, there are cases when  $s_{current}^{pub} = s_{pub}^{last}$  — that is, the last search tree did include the current state.

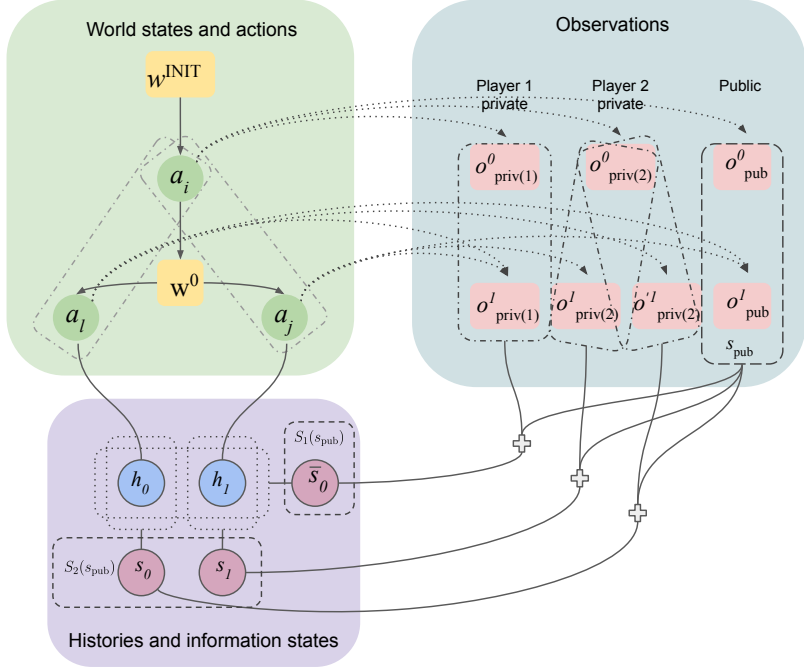


Figure 11: An example of Factored-Observation Stochastic Game (FOSG). This figure presents the visual view of notation from Sec. 2. In this example the game starts in  $w^{init}$  which is the complete state of the environment containing private information for both players. After playing action  $a_i$  the state moves to  $w^0$  where there are two possible actions. Each action emits private and public observations. In this example, actions  $a_j$  and  $a_l$  emit the same private observation  $o^1_{priv(1)}$  for player 1, therefore they cannot distinguish which action happened. On the other hand, player 2 has different observations  $o^1_{priv(2)}$  and  $o'^1_{priv(2)}$  for each of the actions, therefore they have more information about the state of the environment than player 1. The sequence of public observations shared by both players information is denoted as  $s_{pub}$ . Both sequences of actions and factored observations meet in the final 'Histories and information states' view. The two possible action sequences are represented by histories  $h_0$  and  $h_1$ , where  $h_0 = (a_i, a_l)$ ,  $h_1 = (a_i, a_j)$ . Since both actions  $a_l$  and  $a_j$  result in the same observation for player 1, they cannot tell which one of the histories happened and his information state  $\bar{s}_0$  contains them both. This is not the case for player 2, who can separate the histories, and each of his information states  $s_0$  and  $s_1$  contains just one history.

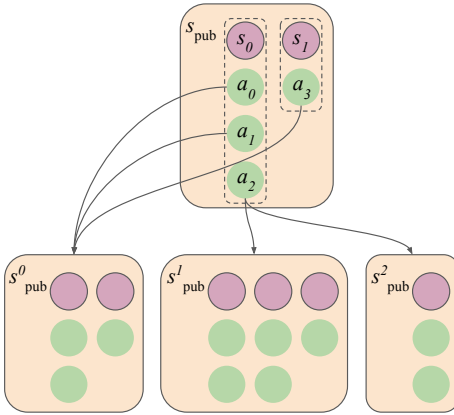


Figure 12: An example of a public tree. The public tree provides different view of the FOSG. In this example actions  $a_0$  and  $a_1$  emit the same public observation and therefore they lead to the same public tree node  $s^0_{pub}$ . On the other hand, action  $a_2$  can lead to multiple possible states, for instance when a detective in Scotland Yard moves to a location the game can either 1) end because Mr. X was there and he was caught or 2) it continues because he was in a different station.

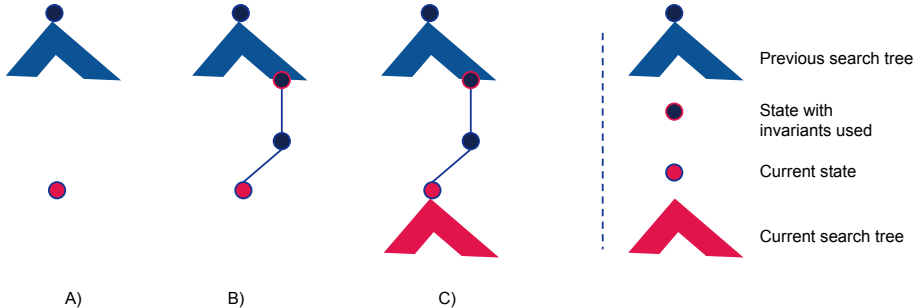


Figure 13: A) The current state might not be included in the previous search tree. In that case, we lack the corresponding invariants to run the re-solving step. B) The re-solving step is rooted in the state that is closest on the path between the last search state and the current state, while being included in the last search tree. C) The expansion process starts its simulations in the current state, expanding the current search tree only under this node.

### B.1.1 Auxiliary (Gadget) Game for Safe Re-Solving

The construction of the re-solving/auxiliary “gadget” game follows [15], where a new state of the opponent is added on top of the subgame. In this state, the opponent can either terminate (T) and receive the constraint values (the re-solving counterfactual values of the opponent), or to follow (F) and play the corresponding subgame. Furthermore, the ranges are used to form the initial distribution of the information states of the player.

Just like DeepStack, the gadget in PoG is further modified by mixing in opponent’s ranges as computed from the previous search  $\beta_s$  (when available). This is achieved by modifying the opponent’s initial ranges in the subgame (distribution over their information states after taking the (F) action).  $\beta'_{follow} = \alpha\beta_{follow} + (1 - \alpha)\beta_s$ . Such mixing has been proven to be sound [55] and empirically improves the performance, and we have chosen  $\alpha = 0.2$ .

## B.2 Complexity of the Algorithm

We now analyse the complexity of the algorithm. Due to size of the network, the network call is substantially expensive operation. We thus analyse how many nodes does an algorithm touch, as well as how many times is the network called. Let  $t$  denote the number of iteration, and  $n_t$  the size of the search tree after  $t$  steps (in terms of public states, assuming the number of information states and histories within a public state is bounded by a constant).

**Expansion Phase** The expansion phase traverses a single trajectory, and uses counterfactual values and CFR policy to drive the tree expansion. At the end of the expansion, a new node is added and then evaluated for its value. If a terminal state is hit at the end of the traversal, there is no expansion. The complexity in terms of the number of neural net calls is thus  $\mathcal{O}(t)$ .

Because the simulation touches every node on the sampled trajectory during the traversal, the number of nodes touched is dependant on the structure of the expanded tree. A degenerate case, where the search tree is always a single path then yields  $\mathcal{O}(n_t) = \mathcal{O}(t)$  for each iteration, resulting in  $\mathcal{O}(t^2)$  worst case. Assuming a well-balanced b-ary tree, each iteration touches only  $\mathcal{O}(\log_b(n_t))$ . Note that this phase is analogous to the MCTS variant employed by AlphaZero and matches its complexity.

**Regret Update Phase** The regret update phase traverses the entire search tree during each iteration, and evaluates the leaf nodes using the value function. As all the nodes  $n_t$  are touched during each iteration, the corresponding complexity is  $\mathcal{O}(t^2)$  regardless of the shape of the tree.

While the number of neural net calls is in general also  $\mathcal{O}(t^2)$ , it is possible to optimize the number of network calls down to  $\mathcal{O}(n_t) = \mathcal{O}(t)$  in any perfect information games (e.g. chess and Go). As the CFR reaches the leaf node, it needs to evaluate  $v_\theta(s_{pub}, r_1, r_2)$  where  $r_i$  represents the reach probabilities of individual information states in the public (leaf) state  $s_{pub}$ . In perfect information games, there is a single information state of each player  $|\mathcal{S}_1(s_{pub})| = |\mathcal{S}_2(s_{pub})| = 1$ . Furthermore, by scaling reach probabilities of player  $i$ , the resulting counterfactual values for player  $-i$  are scaled accordingly. Let  $v_1, v_2 = v_\theta(s_{pub}, r_1, r_2)$ ,  $v'_1, v'_2 = v_\theta(s_{pub}, ar_1, br_2)$ , then  $v'_1 = bv_1, v'_2 = av_2$  for any

$a, b \in \mathcal{R}$ . We can leverage this fact for perfect information games and simply scale the value that was returned by the very first neural net call for that public state. This way, there is only a single network call per public state as subsequent evaluations simply scale the previously returned value. Current implementation of PoG indeed uses this optimization, substantially speeding up the search process.

Currently, PoG uses CFR for the policy improvement and thus needs to traverse the full search tree at each iteration, resulting in  $\mathcal{O}(t^2)$  complexity even for a well balanced tree. There are CFR variants that do not have to traverse the full tree. Namely, MCCFR is a family of sampling based regret minimization methods that only visit and update part of the entire tree and still provide strong convergence guarantees [42]. Outcome sampling is then a particular variant of MCCFR that samples a single trajectory, and thus its complexity matches the expansion phase. While the sampling introduces variances which can slow down the convergence, it is possible to substantially decrease it using the VR-MCCFR method [65].

### B.3 Network Architecture and Optimization

Game	Architecture	Belief features	Public state features
Chess	ResNet	Redundant — there is no uncertainty over players state.	One 8x8 plane for each piece type (6) of each player (2) and repetitions planes (2) for last eight moves + scalar planes (7), 119 8x8 planes in total.
Go	ResNet	Redundant	One 19x19 plane for stones of each player (2) for last eight moves plus a single plane encoding player to act, 17 19x19 planes in total.
Poker	MLP 6 x 2048	1326 (possible private card combinations) * 2 (num of players).	N hot encoding of board cards (52) + commitment of each player normalized by his stack (2) + 1 hot encoding of who acts next, including chance player (3).
Scotland Yard	MLP 6 x 512	1 (detectives' position is always certain) + 199 (possible Mr X's position).	1 hot encoding of position of each detective (5*199) + cards of each detective (5*3) + cards of Mr X (5) + who is playing next (6) + was double move just used (1) + how many rounds were played (1).

Table 2: A neural network architecture and features used for each game.

Table 2 lists neural network architectures and input features used for each game. For chess and Go we use exactly the same architecture and inputs as used by AlphaZero [71]. In poker and Scotland Yard we process concatenated belief and public state features by a MLP with ReLU activations [23].

The counterfactual value head is optimized by Huber loss [32], while policy for each information state  $i$  is optimized by KL divergence:

$$l(\mathbf{v}, \mathbf{p}, \mathbf{v}_{target}, \mathbf{p}_{target}) = w_v * l_{huber}(\mathbf{v}, \mathbf{v}_{target}) + w_p * \sum_i l_{KL}(\pi^i, \pi_{target}^i)$$

where each head is weighted with the corresponding weight  $w_v$  and  $w_p$ . During training we smoothly decay the learning rate by a factor of  $d$  every  $T_{decay}$  steps. Formally learning rate  $\alpha$  at training step  $t$  is defined as:

$$\alpha_t = \alpha_{init} * d^{t/T_{decay}}$$

When using the policy head’s prediction as prior in PUCT formula the logits are processed with softmax with temperature  $T_{prior}$ . This can decrease weight of the prior in some games and encourage more exploration in the search phase.

## B.4 Hyperparameters

Table 3 lists hyperparameters used for each game, most of these parameters are used in algorithms in Section B.5.

Hyperparam	Symbol	Chess	Go	Scot. Yard	HUNL
Batch size		2048	2048	1024	1024
Optimizer		sgd	sgd	sgd	adam
Initial learning rate (LR)	$\alpha_{init}$	0.1	0.02	0.1	0.0001
LR decay steps	$T_{decay}$	40k	200k	2M	2M
LR decay rate	$d$	0.8	0.1	0.5	0.5
Policy head weight	$w_p$	1	1	0.05	0.01
Value head weight	$w_v$	0.25	0.5	1	1
Replay buffer size		50M	50M	1M	1M
Max grad updates per example		1	0.2	5	10
TD(1) target sample probability	$p_{td1}$	0	0.2	0	0
Queries per search	$q_{search}$	1	0	0.3	0.9
Recursive queries per search	$q_{recursive}$	0.2	0	0.1	0.1
Selfplay uniform policy mix	$\epsilon$	0	0	0	0.1
Resign enabled		True	True	False	False
Resign threshold	$resign\_threshold$	-0.9	-0.9	-	-
Min ratio of games without resign	$p_{no\_resign}$	0.2	0.2	-	-
Greedy play after move	$moves_{greedy\_after}$	30	30	never	never
Max moves in one episode	$moves_{max}$	512	722	unlim.	unlim.
Prior softmax temperature	$T_{prior}$	1.5	1.5	1	1

Table 3: Hyperparameters for each game.

## B.5 Pseudocode

Here we provide pseudocode for the most important parts of the PoG algorithm. Algorithm 1 specifies GT-CFR, the core of PoG’s sound game-theoretic search that scales to large perfect information games introduced in Section 3.2. Algorithm 2 presents how GT-CFR is used during selfplay that generates training examples for the neural network, this part was covered in Section 3.4. Hyperparameters used in selfplay are specified in Table 3.

When PoG plays against an opponent the search tree is rebuilt also for the opponent’s actions (as discussed in Section B.1). This way, PoG reasons about the opponent’s behavior since it directly influences the belief distribution for the current state  $\beta$  where PoG is to act.

Note that unlike AlphaZero, PoG currently starts its search procedure from scratch. That is, the previous computation only provides invariants for the next resolving step. AlphaZero rather warm-starts the MCTS process by initializing values and visit counts from the previous search. For PoG, this would also require warm-starting CFR. And while possible [9], there is no warm-starting in the current implementation of PoG.

---

**Algorithm 1** Growing Tree CFR. Note that GT-CFR is logging all neural net queries it does since they might be used later in training.

---

```

procedure GT-CFR( $\mathcal{L}^0, \beta, s, c$ )
     $\triangleright \mathcal{L}^0$  — a tree including  $\beta$  build as described in Sec. B.1.
     $\triangleright \beta$  — a public belief state under which the new nodes will be added.
     $\triangleright s, c$  — total number of expansion simulations and number of simulations per CFR update.
    for  $i \in \{0, 1, \dots, \lceil \frac{s}{c} \rceil - 1\}$  do
         $\text{CFR}(\mathcal{L}^i, \lceil \frac{1}{c} \rceil)$   $\triangleright$  Store average policy and counterfactual values in the tree.
         $\mathcal{L}^{i+1} \leftarrow \text{GROW}(\mathcal{L}^i)$ 
    end for
     $\triangleright$  Return counterfactual values and average policy from CFR and all NN calls.
    return  $\mathbf{v}, \mathbf{p}, nn\_queries$ 
end procedure

procedure GROW( $\mathcal{L}, \beta$ )
    for  $i \in \{0, 1, \dots, \lceil c \rceil - 1\}$  do
         $path \leftarrow \text{SAMPLEPATHDOWNTHETREE}(\mathcal{L}, \beta)$   $\triangleright$  The path starts at  $\beta$ .
         $\text{ADDTOPKCHILDREN}(\mathcal{L}, path, k)$   $\triangleright$  Choice of  $k$  is discussed in Sec. 3.2.2.
         $\text{UPDATEVISITCOUNTSUP}(\mathcal{L}, path)$ 
    end for
    return  $\mathcal{L}$ 
end procedure

```

---

## B.6 Implementation

POG is implemented as a distributed system with decoupled actor and trainer jobs. Each actor runs several parallel games and the neural network evaluations are batched for better accelerator utilization. The networks were implemented using TensorFlow [1].

## B.7 Poker Betting Abstraction

There are up to 20000 possible actions in no-limit Texas hold'em. To make the problem easier, AI agents are typically allowed to use only a small subset of these [55, 13, 7, 85]. This process of selecting a set of allowed actions for a given poker state is called betting abstraction. Even using betting abstraction the players are able to maintain strong performance in the full game [55, 7, 85]. Moreover, the local best response evaluation [47] suggests that there is not an easy exploit for such simplification as long as the agent is able to see full opponent actions [55].

We use a betting abstraction in the Player of Games to speed up the training and simplify the learning task. Our agent's action set was limited to just 3 actions: fold (give up), check/call (match the current wager) and bet/raise (add chips to the pot). To improve generalization we used stochastic betting size similarly to ReBel [7]. The single allowed bet/raise size is randomly uniformly selected at the start of each poker hand from the interval  $\langle 0.5, 1.0 \rangle * pot\_size$ . This amount is anecdotally similar to one used by human players and had also good performance in our experiments. The same random selection was used in both training and evaluation.

As in [7], we have also randomly varied number stack size (number of chips available to the players) at the start of the each round during the training. This number stays fixed during evaluation.

## C Evaluation Details and Additional Experimental Results

### C.1 Description of Leduc poker

Leduc is a simplified poker game with two rounds and a 6-card deck in two suits. Each player initially antes a single chip to play and obtains a single private card and there are three actions: fold, call and raise. There is a fixed bet amount of 2 chips in the first round and 4 chips in the second round, and a limit of two raises per round. After the first round, a single public card is revealed. A pair is the best hand, otherwise hands are ordered by their high card (suit is irrelevant). A player's reward is their gain or loss in chips after the game.

---

**Algorithm 2** Sound Self-play

---

```

procedure SELFPLAY
    Get initial history state  $w \leftarrow w^{INIT}$  and corresponding public state  $\beta$ 
     $\triangleright$  Decide whether the game has to be played till the end.
     $do\_not\_resign \leftarrow$  coin flip with probability  $p_{no\_resign}$ 
    while  $w$  is not terminal AND played less than  $moves_{max}$  do
        if chance acts in  $w$  then
             $a \leftarrow$  uniform random action.
        else
             $\triangleright$  POG acts for all non-chance players.
             $v_w, \pi_w^{controller} \leftarrow \text{POGSELFPLAYCONTROLLER}(w)$ 
            if  $v_w < resign\_threshold$  AND  $not(do\_not\_resign)$  then
                 $\triangleright$  Don't waste compute on already decided game.
                return
            end if
             $\triangleright$  Mix controller's policy with uniform prior to encourage exploration.
             $\pi_w^{selfplay} \leftarrow (1 - \epsilon) \cdot \pi_w^{controller} + \epsilon \cdot \pi^{uniform}$ 
            if moves played  $< moves_{greedy\_after}$  then
                 $a \leftarrow$  sample action from  $\pi_w^{selfplay}$ 
            else
                 $a \leftarrow \arg \max \pi_w^{selfplay}$ 
            end if
        end if
         $w \leftarrow$  apply action  $a$  on state  $w$ 
    end while
     $\triangleright$  Sampling states with TD(1) targets.
    for each belief state  $\beta \in$  played trajectory  $tr$  do
        if uniform random sample from unit interval  $< p_{td1}$  then
             $\mathbf{v} \leftarrow$  outcome of  $tr$  assigned to information state visited in  $\beta$ 
             $\mathbf{p} \leftarrow$  policy used in  $\beta$ 
            replay_buffer.append( $(\beta, (\mathbf{v}, \mathbf{p}))$ )
        end if
    end for
end procedure

procedure POGSELFPLAYCONTROLLER( $w$ )
     $\beta \leftarrow$  public state including  $w$ 
     $\mathcal{L} \leftarrow$  the tree including  $\beta$  build as described in Sec. B.1.
     $\mathbf{v}, \mathbf{p} \leftarrow \text{TRAINING-GT-CFR}(\mathcal{L})$ 
    return  $\mathbf{v}(w), \mathbf{p}(w)$ 
end procedure

procedure TRAINING-GT-CFR( $\mathcal{L}$ )
     $\mathbf{v}, \mathbf{p}, nn\_queries \leftarrow \text{GT-CFR}(\mathcal{L})$ 
    queries  $\leftarrow$  Pick on average  $q_{search}$  neural net queries  $\beta$  from  $nn\_queries$ .
    queries_to_solve.extend(queries)
    return  $\mathbf{v}, \mathbf{p}$ 
end procedure

procedure QUERYSOLVER
    for  $\beta \leftarrow$  queries_to_solve.pop() do
         $\mathbf{v}, \mathbf{p}, nn\_queries \leftarrow \text{GT-CFR}(\beta)$ 
         $\triangleright$  Send the example to the trainer.
        replay_buffer.append( $(\beta, (\mathbf{v}, \mathbf{p}))$ )
         $\triangleright$  Create recursive queries.
        queries  $\leftarrow$  Pick on average  $q_{recursive}$  neural net queries  $\beta$  from  $nn\_queries$ .
        queries_to_solve.extend(queries)
    end for
end procedure

```

---

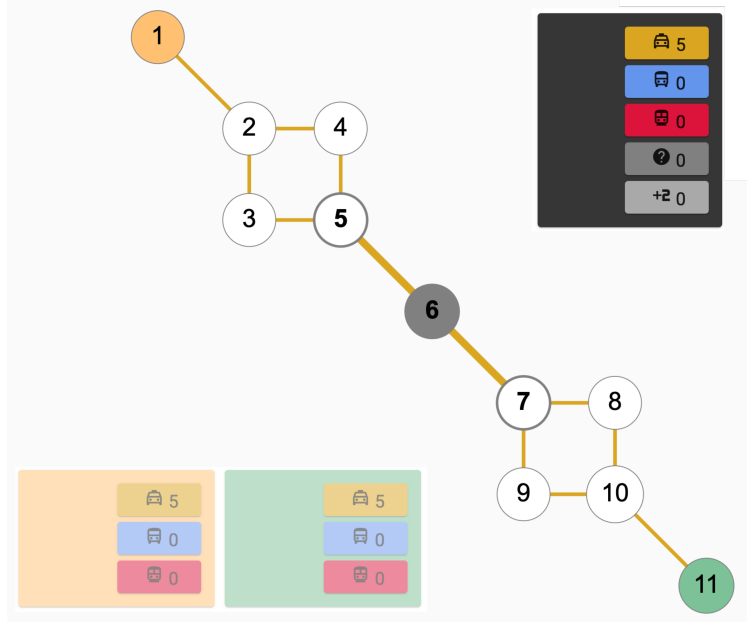


Figure 14: Initial situation on the glasses map for Scotland Yard. Mr. X starts at station 6 while the two detectives start at stations 1 and 11. All of them have 5 taxi cards (all edges in this map are of the same type) and the game is played for 5 rounds.

## C.2 Custom Glasses Map for Scotland Yard

Figure 14 shows the layout and describes the custom “glasses” map for Scotland Yard.

## C.3 Full Results of Go Agent Tournament

Full performance results of the Go tournament are shown in Table 4.

## C.4 Reinforcement Learning and Search in Imperfect Information Games

In this section, we provide some experimental results showing that common RL and widely-used search algorithms can produce highly exploitable strategies, even in small imperfect information games where exploitability is computable exactly. In particular, we show how exploitable Information Set Monte Carlo Tree Search is in Leduc poker, as well as three standard RL algorithms (DQN, A2C and tabular Q-learning) in both Kuhn poker and Leduc poker using OpenSpiel [41].

### C.4.1 Information Set Monte Carlo Tree Search

Information Set Monte Carlo Tree Search (IS-MCTS) is a search method that, at the start of each simulation, first samples a world state—consistent with the player’s information state—and uses it for the simulation [19]. Reward and visit count statistics are aggregated over information states so that players base their decisions only on their information states rather than on private information inaccessible to them.

Figure 5 shows the exploitability of a policy obtained by running separate independent IS-MCTS searches from each information state in the game, over various parameter values. The lowest exploitability of IS-MCTS we found among this sweep was **465 mbb/h**.

### C.4.2 Standard RL algorithms in Imperfect Information Games

As imperfect information games generally need stochastic policies to achieve an optimal strategy, one might wonder how exploitable standard RL algorithms are in this class of games. To test this, we trained three standard RL agents: DQN, policy gradient (A2C) and tabular Q-learning. We used MLP neural networks in DQN and A2C agents. Table 6 shows the hyper parameters we swept over to train these RL agents.

In Kuhn poker, the best performing A2C agent converges to exploitability of 52 mbb/h, and tabular Q-learning and DQN agents converge to around 250 mbb/h. Similarly, in Leduc poker, the

Agent	Rel. Elo
AlphaZero(s=16k, t=800k)	+3139
AlphaZero(s=16k, t=400k)	+3021
AlphaZero(s=8k, t=800k)	+2875
AlphaZero(s=8k, t=400k)	+2801
AlphaZero(s=4k, t=800k)	+2643
AlphaZero(s=16k, t=200k)	+2610
AlphaZero(s=4k, t=400k)	+2584
AlphaZero(s=2k, t=800k)	+2451
AlphaZero(s=8k, t=200k)	+2428
AlphaZero(s=2k, t=400k)	+2353
AlphaZero(s=4k, t=200k)	+2234
AlphaZero(s=800, t=800k)	+2099
AlphaZero(s=16k, t=100k)	+2088
AlphaZero(s=2k, t=200k)	+2063
AlphaZero(s=800, t=400k)	+2036
<b>PoG(s=16k, c=10)</b>	<b>+1970</b>
AlphaZero(s=8k, t=100k)	+1940
<b>PoG(s=8k, c=10)</b>	<b>+1902</b>
AlphaZero(s=800, t=200k)	+1812
<b>PoG(s=4k, c=10)</b>	<b>+1796</b>
AlphaZero(s=4k, t=100k)	+1783
<b>PoG(s=2k, c=10)</b>	<b>+1672</b>
AlphaZero(s=2k, t=100k)	+1618
<b>PoG(s=800, c=1)</b>	<b>+1426</b>
AlphaZero(s=800, t=100k)	+1360
Pachi(s=100k)	+869
Pachi(s=10k)	+231
GnuGo(l=10)	+0

Table 4: Full Go results. Elo of GnuGo with a single thread and 100ms thinking time was set to be 0. AlphaZero(s=16k, t=800k) refers to 16000 search simulations.

best performing A2C agent converges to exploitability of 78 mbb/h, tabular Q-learning and DQN agents converge to about 1300 mbb/h and 900 mbb/h respectively. Figure 15 shows the exploitability of RL agents in Kuhn poker and Leduc poker.

## D Scotland Yard example

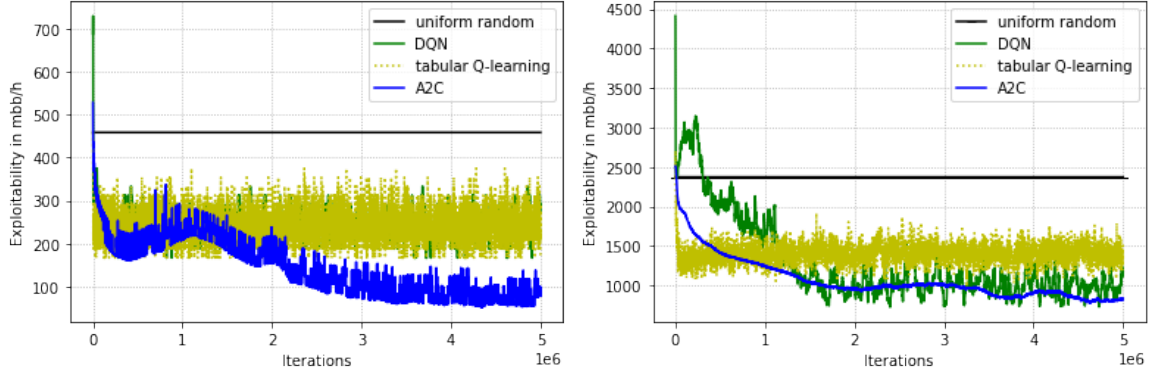
Figure 16 describes an example situation from Scotland Yard.

Num. Sims	UCT const. ( $C$ )	Expl. (mvd)	Expl. (mvis)	Expl. (mval)
10	1.0	2168	2449	2173
10	2.0	2058	2408	2341
10	5.0	1902	2615	2517
10	10.0	1738	2555	2360
10	13.0	1799	2517	2598
10	20.0	1821	2830	2349
10	26.0	1888	2861	2669
100	1.0	1489	1509	1333
100	2.0	1404	1587	1395
100	5.0	1239	1145	1094
100	10.0	1213	1195	1245
100	13.0	1218	1292	1227
100	20.0	1350	1456	1342
100	26.0	1448	1747	1568
1000	1.0	1323	1218	1177
1000	2.0	1069	1212	864
1000	5.0	699	778	681
1000	10.0	697	601	632
1000	13.0	741	759	744
1000	20.0	859	962	991
1000	26.0	966	1029	1057
10000	1.0	1348	948	1134
10000	2.0	911	877	763
10000	5.0	516	582	538
10000	10.0	490	485	480
10000	13.0	511	465	470
10000	20.0	572	505	505
10000	26.0	631	575	570

Table 5: Average exploitability (in mbb/h) over five policy constructions obtained by independent searches of IS-MCTS runs at each information state in Leduc Poker. The parameter  $C$  is the value of the UCT exploration constant. The final policy is obtained either by normalizing the visit counts (mvd), choosing the action with maximum visits (mvis), or choosing the action with the maximal Monte Carlo value estimate (mval).

Parameter	DQN	Tabular Q-Learning	A2C
Learning rate (lr)	1e-1, 1e-2, 1e-3, 1e-4	NA	Actor lr: 1e-3, 1e-4, 1e-5 Critic lr: 1e-2, 1e-3
Decaying exploration rate	1., 0.8, 0.5, 0.2, 0.1	NA	NA
Replay buffer size	100, 1000, 10000, 100000	NA	NA
Hidden layer size	'32', '64', '128', '32', '32', '64', '64'	NA	'32', '64', '128', '32', '32', '64', '64'
Num. of critic updates before every actor update	NA	NA	4, 8, 16
Step size	NA	0.1, 0.2, 0.5, 0.8, 1.0	

Table 6: Hyper parameters swept over in each RL algorithm.



(a) Exploitability in 2-player Kuhn poker

(b) Exploitability in 2-player Leduc poker

Figure 15: Comparing performance of DQN, A2C, tabular Q-learning and uniform random policy in (a) Kuhn poker and (b) Leduc poker

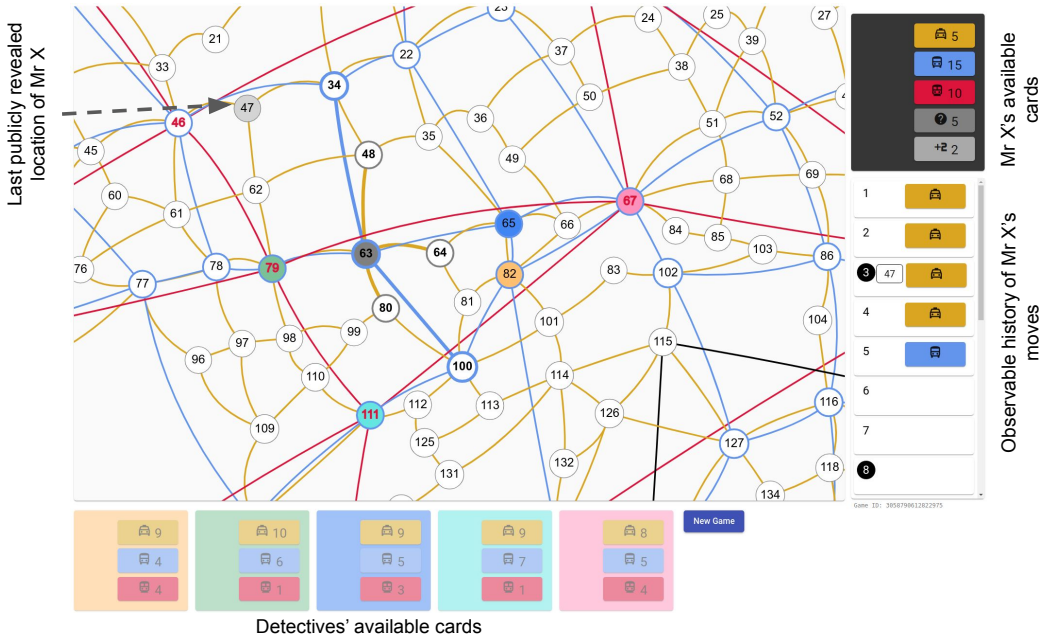


Figure 16: An example situation in Scotland Yard. The centre shows a game map abstracted as a graph with different types of edges (yellow for taxi, blue for bus, red for subway and black for boat). Both the detectives and Mr. X have corresponding cards that allow them to move edges of the same type. In the current situation, the game is in round 5 and Mr. X is to act. He is in location 63, however the detectives (locations 65, 67, 79, 82 and 111) saw his exact location last time in round 3 when he was in location 47 (he will have to reveal himself again in rounds 8, 13, 18 and the final round 24). Since then the detectives observed just the type of the edge Mr. X moved along (in this case taxi and bus) and they have to "guess" where he is and subsequently where he is going to be in order to catch him. While Mr. X is hidden locations of detectives are public. In single move Mr. X can get to locations 48, 64 or 80 by taxi and to locations 34 or 100 by bus. He can use a card of the corresponding colour (taxi or bus) however that will give unwanted hint to the detectives. He can also use "?" card (he has 5 at the moment) that hides his mode of transport, therefore it increases detectives' uncertainty about his location. Finally, he can use double move card (he has only 2) that would allow him to do two moves instead of one.

## E Proofs of Theorems

There are three substantive differences between the PoG algorithm and DeepStack. First, PoG uses a growing search tree, rather than using a fixed limited-lookahead tree. Second, the PoG search tree may depend on the observed chance events. Finally, PoG uses a continuous self-play training loop operating throughout the entire game, rather than the stratified bottom-up training process used by DeepStack. We address each of these differences below, in turn, after considering how to describe an approximate value function for search in imperfect information games.

### Value Functions for Subgames

Like DeepStack, the PoG algorithm uses a value function, so the quality of its play depends on the quality of the value function. We will describe a value function in terms of its distance to a strategy with low regret. We start with some value and regret definitions that are better suited to subgames.

Consider some strategy profile  $\pi$  which is a tuple containing a strategy for each player, public tree subgame  $S$  rooted at public state  $s_{\text{pub}}$  with player range vectors  $B_i[s_i \in \mathcal{S}_i(s_{\text{pub}})] := P_i(s_i|\pi)$ . First, note that we can re-write counterfactual value  $v$  so that it depends only on  $B$  and  $\pi$  restricted to  $S$ , with no further dependence on  $\pi$ . Let  $s_i$  be a Player  $i$  information state in  $\mathcal{S}_i(s_{\text{pub}})$ , and  $q$  be the opponent of Player  $i$ , then:

$$\begin{aligned} v^{B,\pi^S}(s_i) &:= \sum_{h \in I(s_i)} \sum_{z \sqsupset h} B_q[s_q(h)] P_c(h) P(z|h, \pi^S) u_i(z) \\ &= \sum_{h \in I(s_i)} \sum_{z \sqsupset h} P_{-p}(h|\pi) P(z|h, \pi) u_i(z) = v^\pi(s_i) \end{aligned}$$

We can write a number of quantities in terms of the best-response value at information state  $s_i$ :

$$BV^{B,\pi^S}(s_i) := \max_{\pi_i^*} v^{B,\pi^S \leftarrow \pi_i^*}(s_i)$$

where  $\pi \leftarrow \pi'$  is the strategy profile constructed by replacing action probabilities in  $\pi$  with those in  $\pi'$ . The value function is a substitute for an entire subgame strategy profile, so the regret we are interested in is player  $i$ 's full counterfactual regret [86] at  $s_i$ , which considers all possible strategies within subgame  $S$ :

$$R_{s_i}^{\text{full}}(B, \pi^S) := BV^{B,\pi^S}(s_i) - v^{B,\pi^S}(s_i)$$

With these definitions in hand, we can now consider the quality of a value function  $f$  in terms of a regret bound  $\epsilon$  and value error  $\xi$ . Recall that  $f$  maps ranges  $B$  and public state  $s_{\text{pub}}$  to a vector of values  $\tilde{v}(s_i)$  for each player  $i$ .

First, we consider versions of the regret bound and value error which are parameterised by a strategy  $\pi$ . There is some associated bound  $\epsilon(\pi)$  on the sum of regrets across all information states at any subgame, valid for both players.

$$\epsilon(\pi) := \max_B \max_{s_{\text{pub}}} \max_i \sum_{s_i \in \mathcal{S}_i(s_{\text{pub}})} R_{s_i}^{\text{full}}(B, \pi)$$

There is also some bound  $\xi_f(\pi)$  on the distance between  $f(s_{\text{pub}}, B)$  and the best-response values to  $\pi$ .

$$\xi_f(\pi) := \max_B \max_{s_{\text{pub}}} \max_i \sum_{s_i \in \mathcal{S}_i(s_{\text{pub}})} |f(s_{\text{pub}}, B)[s_i] - v^{B,\pi}(s_i)|$$

We then say that  $f$  has  $\epsilon, \xi$  quality bounds if there exists some strategy  $\pi$  such that  $\epsilon(\pi) \leq \epsilon$  and  $\xi_f(\pi) \leq \xi$ . As desired, if both  $\epsilon$  and  $\xi$  are low then  $f(s_{\text{pub}}, B)$  is a good approximation of the best-response values to a low-regret strategy, for a subgame rooted at  $s_{\text{pub}}$  with initial beliefs  $B$ .

The DeepStack algorithm [55] used a similar error metric for value functions, but only considered zero-regret strategies. We introduce a more complicated error measure because the space of values corresponding to low-regret strategies may be much larger than the space of values corresponding to no-regret strategies. For example, consider the public subgame of a matching pennies game after the first player acts with the policy 0.501 heads, 0.499 tails. There are two first-player information states, from playing either heads or tails, with an empty first-player strategy as there are no further

first player actions. Let us assume a value function  $f$  is returning the values  $[0 \ 0]$  for these two information states. How good is  $f$ , assuming we restrict our attention to this one subgame?

The unique zero-regret strategy for the second player is to play tails 100% of the time, resulting in first player counterfactual values of -1 for playing heads and 1 for playing tails. The error metric based on zero-regret strategies is therefore measuring  $|f([0.501 \ 0.499]) - [-1 \ 1]|_1$ , so that the DeepStack metric states that  $f$  has an error of 2. However,  $[0 \ 0]$  seems like a very reasonable choice: these are exactly the first player counterfactual values when the second player has a strategy of 0.5 heads, 0.5 tails, which has a regret of only 0.002 in this subgame. Rather than saying  $f$  is a poor quality value function with an error of 2 in a game with utilities in  $[-1, 1]$ , we can now say  $f$  is a great 0.002, 0 value function which exactly describes a low-regret strategy.

The new quality metric also addresses an issue the old DeepStack metric had with discontinuities in the underlying 0-regret value functions. This means that the space of functions with a low DeepStack error metric may not be well suited for learning from data. Continuing with the previous example, if we shifted  $B$  slightly to be 0.499 heads and 0.501 tails for the first player, the unique 0-regret strategy in the subgame flips to playing tails 0% of the time, while the uniform random strategy is still a low-regret strategy for this subgame. In this example, a function can only have a low error with the DeepStack metric if it accurately predicts the values everywhere around the discontinuity at 0.5 heads and 0.5 tails, whereas the new metric can avoid this discontinuity by picking an  $\epsilon > 0$ . More generally, for any constant  $c$ , the objective  $\epsilon + c\xi$  is a continuous function in  $B$ , making it a potentially more attractive learning target than the discontinuous function defined by exact Nash equilibrium values, and which matches a learning procedure based on approximately solving example subgames.

## Growing Trees

One major step in showing soundness of the PoG algorithm is demonstrating that Growing Tree CFR (GT-CFR) can approximately solve games. As a quick recap, GT-CFR is a variant of the CFR algorithm [86] that uses limited lookahead and a value function, storing values within a tree that grows over time, in a fashion similar to UCT [39]. We use this new algorithm as a component to solve the problems that the PoG algorithm sets up. At every non-terminal public leaf state  $s_{\text{pub}}$  of the lookahead tree, GT-CFR uses estimated counterfactual values  $\tilde{v}$ , generated from a value function  $f(s_{\text{pub}}, B)$  with player ranges  $B$  induced by Bayes' rule at  $s_{\text{pub}}$  for the current strategy profile  $\pi$ .

Like DeepStack, PoG has two steps which involve solving subgames of the original game. One of the steps is the re-solving step used to play through a game, where we solve a modified subgame based on constraints on opponent values and beliefs about our possible private information, in order to get our policy and new opponent values. The other step is only in the training loop, where we are solving a subgame with fixed beliefs for both players, in order to get values for both players. While the (sub)games for these two cases are slightly different, they are both well-formed games and we can find an approximate Nash equilibrium using GT-CFR.

When running GT-CFR, even though a policy is explicitly defined only at information states in the lookahead tree  $\mathcal{L}$ , at each iteration  $t$  there is implicitly some complete strategy profile  $\pi^t$ . For any information state  $s$  in  $\mathcal{L}$  which is not a leaf,  $\pi^t(s)$  is explicitly defined by the regret-matching policy. For all other  $s$  – either a leaf of  $\mathcal{L}$  or outside of the lookahead tree –  $\pi^t(s)$  is defined by the  $\epsilon$ -regret subgame strategy profile  $\pi^{*,S}$  associated with the value function's  $\epsilon, \xi$  quality bounds. Note that this  $\pi^t$  only exists as a concept which is useful for theoretical analysis: GT-CFR does not have access to the probabilities outside of its lookahead tree, only a noisy estimate of the associated counterfactual values provided by the value function.

**Lemma 1.** *Let  $p$  and  $q$  be vectors in  $[0, 1]^n$ , and  $v$  and  $w$  be vectors in  $\mathbb{R}^n$  such that  $v[i] > w[i]$  for all  $i$ . Then  $p \cdot v - q \cdot w \leq \mathbf{1} \cdot (v - w) + p \cdot w - q \cdot w$*

*Proof.*

$$\begin{aligned} p \cdot v - q \cdot w &= p \cdot v - p \cdot w + p \cdot w - q \cdot w \\ &= p \cdot (v - w) + p \cdot w - q \cdot w \\ &\leq \mathbf{1} \cdot (v - w) + p \cdot w - q \cdot w \end{aligned}$$

□

**Lemma 2.** *Let  $p$  and  $q$  be vectors in  $[0, 1]^n$ , and  $v$  and  $w$  be vectors in  $\mathbb{R}^n$  such that  $\sum_{i=1}^n |v[i] - w[i]| \leq \xi$ . Then  $(p - q) \cdot v \leq \xi + (p - q) \cdot w$ .*

*Proof.*

$$\begin{aligned}
(p - q) \cdot v &= (p - q) \cdot (v - w) + (p - q) \cdot w \\
&\leq \sum_{i=1}^n |(p[i] - q[i])(v[i] - w[i])| + (p - q) \cdot w \\
&\leq \sum_{i=1}^n |(v[i] - w[i])| + (p - q) \cdot w \\
&\leq \xi + (p - q) \cdot w
\end{aligned}$$

□

In GT-CFR, the depth-limited public tree used for search may change at each iteration. Let  $\mathcal{L}^t$  be the public tree at time  $t$ . For any given tree  $\mathcal{L}$ , let  $\mathcal{N}(\mathcal{L})$  be the interior of the tree: all non-leaf, non-terminal public states. The interior of the tree is where regret matching is used to generate a policy, with regrets stored for all information states in interior public states. Let  $\mathcal{F}(\mathcal{L})$  be the frontier of  $\mathcal{L}$ , containing non-terminal leaves, and  $\mathcal{Z}(\mathcal{L})$  be the terminal public states. GT-CFR uses the value function at all public states in the frontier, receiving noisy estimates  $\tilde{v}(s)$  of the true counterfactual values  $v(s)$ . We will distinguish between the true regrets  $R_s^T$  computed from the entire policy, and the regret  $\tilde{R}_s^T$  computed using the estimated values  $\tilde{v}(s)$ . Given a sequence of trees across  $T$  iterations, let  $\mathcal{T}_n(s_{\text{pub}})$  be the set of maximal length intervals  $[a, b] \subseteq [1, T]$  where  $s_{\text{pub}}$  is in  $\mathcal{N}(\mathcal{L}^t)$  for all  $t \in [a, b]$ . Let  $U$  be the maximum difference in counterfactual value between any two strategies, at any information state, and  $A$  be the maximum number of actions at any information state.

**Lemma 3.** *After running GT-CFR for  $T$  iterations starting at some initial public state  $s_0$ , using a value function with quality  $\epsilon, \xi$ , regret for the strategies satisfies the bound*

$$\begin{aligned}
\sum_{s_i \in \mathcal{S}_i(s_0)} R_{s_i}^T &\leq \sum_{t=1}^T |\mathcal{F}(\mathcal{L}^t)|(\epsilon + \xi) \\
&\quad + \sum_{s_{\text{pub}} \in \bigcup_{t=1}^T \mathcal{L}^t} |\mathcal{S}_i(s_{\text{pub}})|U\sqrt{A} \sum_{[a,b] \in \mathcal{T}_n(s_{\text{pub}})} \sqrt{|[a,b]|}
\end{aligned}$$

*Proof.* Starting with the definition of regret, and noting that regrets are independently maximised in a perfect recall game, we can rearrange terms to get

$$\begin{aligned}
\sum_{s_i \in \mathcal{S}_i(s_0)} R_{s_i}^T &= \sum_{s_i \in \mathcal{S}_i(s_0)} \left( \max_{\pi_i^*} \sum_{t=1}^T v^{\pi^t \leftarrow \pi_i^*}(s_i) - \sum_{t=1}^T v^{\pi^t}(s_i) \right) \\
&= \max_{\pi_i^*} \sum_{s_i \in \mathcal{S}_i(s_0)} \left( \sum_{t=1}^T v^{\pi^t \leftarrow \pi_i^*}(s_i) - \sum_{t=1}^T v^{\pi^t}(s_i) \right) \\
&= \max_{\pi_i^*} \sum_{t=1}^T \sum_{s_i \in \mathcal{S}_i(s_0)} \left( v^{\pi^t \leftarrow \pi_i^*}(s_i) - v^{\pi^t}(s_i) \right)
\end{aligned}$$

We can rewrite the counterfactual values of information state  $s_i$  in terms of the counterfactual value of leaves and terminals of the tree.

$$\begin{aligned}
&= \max_{\pi_i^*} \sum_{t=1}^T \left( \sum_{s_{\text{pub}} \in \mathcal{F}(\mathcal{L}^t)} \sum_{s_i \in \mathcal{S}_i(s_{\text{pub}})} \left( P_i(s_i | \pi_i^*) v^{\pi^t \leftarrow \pi_i^*}(s_i) - P_i(s_i | \pi^t) v^{\pi^t}(s_i) \right) \right. \\
&\quad \left. + \sum_{s_{\text{pub}} \in \mathcal{Z}(\mathcal{L}^t)} \sum_{z \in I(s_{\text{pub}})} \left( P_i(z | \pi^t \leftarrow \pi_i^*) v^{\pi^t}(z) - P_i(z | \pi^t) v^{\pi^t}(z) \right) \right) \quad (1)
\end{aligned}$$

Examining part of the first term inside the sum, we can independently maximise the counterfactual values at each information state  $s_i$ . As above, this is equivalent to maximising at public state  $s_{\text{pub}}$ .

$$\begin{aligned} & \sum_{s_i \in \mathcal{S}_i(s_{\text{pub}})} \left( P_i(s_i | \pi_i^*) v^{\pi^t \leftarrow \pi_i^*}(s_i) - P_i(s_i | \pi^t) v^{\pi^t}(s_i) \right) \\ & \leq \sum_{s_i \in \mathcal{S}_i(s_{\text{pub}})} \max_{\pi^{**}} \left( P_i(s_i | \pi_i^*) v^{\pi^t \leftarrow \pi_i^{**}}(s_i) - P_i(s_i | \pi^t) v^{\pi^t}(s_i) \right) \\ & = \max_{\pi^{**}} \sum_{s_i \in \mathcal{S}_i(s_{\text{pub}})} \left( P_i(s_i | \pi_i^*) v^{\pi^t \leftarrow \pi_i^{**}}(s_i) - P_i(s_i | \pi^t) v^{\pi^t}(s_i) \right) \end{aligned}$$

Given that we individually maximised over each minuend, we satisfy the requirements of Lemma 1. We can then use the value function quality bounds.

$$\begin{aligned} & \leq \max_{\pi^{**}} \sum_{s_i \in \mathcal{S}_i(s_{\text{pub}})} \left( v^{\pi^t \leftarrow \pi_i^{**}}(s_i) - v^{\pi^t}(s_i) \right) \\ & + \sum_{s_i \in \mathcal{S}_i(s_{\text{pub}})} \left( P_i(s_i | \pi_i^*) v^{\pi^t}(s_i) - P_i(s_i | \pi^t) v^{\pi^t}(s_i) \right) \\ & \leq \epsilon + \sum_{s_i \in \mathcal{S}_i(s_{\text{pub}})} \left( P_i(s_i | \pi_i^*) v^{\pi^t}(s_i) - P_i(s_i | \pi^t) v^{\pi^t}(s_i) \right) \end{aligned}$$

Up to this point, we have used the true counterfactual values for the current strategy profile. At leaves, however, GT-CFR only has access to the value function's noisy estimates of the true values. Applying Lemma 2, we get

$$\leq \epsilon + \xi + \sum_{s_i \in \mathcal{S}_i(s_{\text{pub}})} \left( P_i(s_i | \pi_i^*) \tilde{v}^{\pi^t}(s_i) - P_i(s_i | \pi^t) \tilde{v}^{\pi^t}(s_i) \right)$$

Placing this back into line 1 and collecting  $\epsilon$  and  $\xi$  terms, we have

$$\begin{aligned} \sum_{s_i \in \mathcal{S}_i(s_0)} R_{s_i}^T & \leq \sum_{t=1}^T |\mathcal{F}(\mathcal{L}^t)|(\epsilon + \xi) + \max_{\pi_i^*} \sum_{t=1}^T \\ & \left( \sum_{s_{\text{pub}} \in \mathcal{F}(\mathcal{L}^t)} \sum_{s_i \in \mathcal{S}_i(s_{\text{pub}})} \left( P_i(s_i | \pi_i^*) \tilde{v}^{\pi^t}(s_i) - P_i(s_i | \pi^t) \tilde{v}^{\pi^t}(s_i) \right) \right. \\ & \left. + \sum_{s_{\text{pub}} \in \mathcal{Z}(\mathcal{L}^t)} \sum_{z \in I(s_{\text{pub}})} \left( P_i(z | \pi^t \leftarrow \pi_i^*) v^{\pi^t}(z) - P_i(z | \pi^t) v^{\pi^t}(z) \right) \right) \end{aligned}$$

We can rearrange the sums to consider the regret contribution for each public state

$$\begin{aligned} & = \sum_{t=1}^T |\mathcal{F}(\mathcal{L}^t)|(\epsilon + \xi) + \max_{\pi_i^*} \sum_{s_{\text{pub}} \in \bigcup_{t=1}^T \mathcal{L}^t} \\ & \left( \sum_{t \text{ s.t. } s_{\text{pub}} \in \mathcal{F}(\mathcal{L}^t)} \sum_{s_i \in \mathcal{S}_i(s_{\text{pub}})} \left( P_i(s_i | \pi_i^*) \tilde{v}^{\pi^t}(s_i) - P_i(s_i | \pi^t) \tilde{v}^{\pi^t}(s_i) \right) \right. \\ & \left. + \sum_{t \text{ s.t. } s_{\text{pub}} \in \mathcal{Z}(\mathcal{L}^t)} \sum_{z \in I(s_{\text{pub}})} \left( P_i(z | \pi^t \leftarrow \pi_i^*) v^{\pi^t}(z) - P_i(z | \pi^t) v^{\pi^t}(z) \right) \right) \end{aligned}$$

As before we can use Lemma 1 to separate out regrets at the interior states in  $\mathcal{N} := \mathcal{F}(\mathcal{N}(\bigcup_{t=1}^T \mathcal{L}^t))$ , which always depend only on leaves and terminals. Let  $\mathcal{L}'^t$  be  $\mathcal{L}^t$  minus all public states in  $\mathcal{N}$  and

any successor states.

$$\begin{aligned}
&\leq \sum_{t=1}^T |\mathcal{F}(\mathcal{L}^t)|(\epsilon + \xi) + \sum_{s_{\text{pub}} \in \mathcal{N}} \sum_{[a,b] \in \mathcal{T}_n(s_{\text{pub}})} \sum_{s_i \in s_{\text{pub}}} \tilde{R}_{s_i}^{a,b} + \max_{\pi_i^*} \sum_{s_{\text{pub}} \in \bigcup_{t=1}^T \mathcal{L}'^t} \\
&\quad \left( \sum_{t \text{ s.t. } s_{\text{pub}} \in \mathcal{F}(\mathcal{L}'^t)} \sum_{s_i \in \mathcal{S}_i(s_{\text{pub}})} \left( P_i(s_i | \pi_i^*) \tilde{v}^{\pi^t}(s_i) - P_i(s_i | \pi^t) \tilde{v}^{\pi^t}(s_i) \right) \right. \\
&\quad \left. + \sum_{t \text{ s.t. } s_{\text{pub}} \in \mathcal{Z}(\mathcal{L}'^t)} \sum_{z \in I(s_{\text{pub}})} \left( P_i(z | \pi^t \leftarrow \pi_i^*) v^{\pi^t}(z) - P_i(z | \pi^t) v^{\pi^t}(z) \right) \right)
\end{aligned}$$

Note that the states which were separated out are now effectively terminals in smaller trees. We can repeat this process until regrets for all public states have been separated out.

$$\leq \sum_{t=1}^T |\mathcal{F}(\mathcal{L}^t)|(\epsilon + \xi) + \sum_{s_{\text{pub}} \in \bigcup_{t=1}^T \mathcal{L}^t} \sum_{[a,b] \in \mathcal{T}_n(s_{\text{pub}})} \sum_{s_i \in s_{\text{pub}}} \tilde{R}_{s_i}^{a,b}$$

Finally, from bounds on regret-matching[27],

$$\leq \sum_{t=1}^T |\mathcal{F}(\mathcal{L}^t)|(\epsilon + \xi) + \sum_{s_{\text{pub}} \in \bigcup_{t=1}^T \mathcal{L}^t} |\mathcal{S}_i(s_{\text{pub}})| U \sqrt{A} \sum_{[a,b] \in \mathcal{T}_n(s_{\text{pub}})} \sqrt{|[a,b]|}$$

□

Note that the form of Lemma 3 implies that regret might not be sub-linear if public states are repeatedly added and removed from the lookahead tree. If we only add states and never remove them, however, we get a standard CFR regret bound plus error terms for the value function.

**Theorem 3.** *Assume the conditions of Lemma 3 hold, and public states are never removed from the lookahead tree. Then*

$$R_i^{T,\text{full}} \leq \sum_{t=1}^T |\mathcal{F}(\mathcal{L}^t)|(\epsilon + \xi) + \sum_{s_{\text{pub}} \in \mathcal{N}(\mathcal{L}^T)} |\mathcal{S}_i(s_{\text{pub}})| U \sqrt{AT}$$

*Proof.* This follows from Lemma 3, noting that the interior of  $\mathcal{L}^t$  monotonically grows over time. □

## Self-play Values as Re-solving Constraints

By using a value network in solving, we lose the ability to compute our opponent's counterfactual best response values to our average strategy [78]. It is easy to track the opponent's average self-play value across iterations of a CFR variant, but using these values as re-solving constraints does not trivially lead to a bound on exploitability for the re-solved strategy. We show here that average CFR self-play values lead to reasonable, controllable error bounds in the context of continual re-solving. We will use  $(x)^+$  to mean  $\max\{x, 0\}$ . For simplicity, we will also assume that the subgame that is being re-solved is in the GT-CFR lookahead tree for all iterations.

**Theorem 4.** *Assume we have some average strategy  $\bar{\pi}$  generated by  $T$  iterations of GT-CFR solver using a value function with quality  $\epsilon, \xi$ , with final lookahead tree  $\mathcal{L}^T$  where public states were never removed from the lookahead tree, and a final average regret  $R_i^T$  for the player of interest. Further assume that we have re-solved some public subgame  $S$  rooted public state  $s_{\text{pub}}$ , using the average counterfactual values  $\bar{v}(s_o) := \frac{1}{T} \sum_{t=1}^T v^{\pi^t}(s_o)$  as the opt-out values in the re-solving gadget. Let  $\pi^S$  be the strategy generated from the re-solving game, with some player and opponent average regrets  $\bar{R}_i^S$  and  $\bar{R}_o^S$ , respectively. Then*

$$\begin{aligned}
BV_o^{\bar{\pi} \leftarrow \pi^S} - BV_o^{\bar{\pi}} &\leq (\bar{R}_o^S)^+ + (\bar{R}_i^S)^+ + \bar{R}_i \\
&\quad + 2 \left( \max_t |\mathcal{F}(\mathcal{L}_{s_{\text{pub}}}^t)|(\epsilon + \xi) + \sum_{s_{\text{pub}} \in \mathcal{N}(\mathcal{L}_{s_{\text{pub}}}^T)} |\mathcal{S}_i(s_{\text{pub}})| U \sqrt{\frac{A}{T}} \right)
\end{aligned}$$

*Proof.* The general outline of the proof has two parts, both asking the question "how much can the opponent best response value increase?" As in Lemma 4 of [55], we can consider breaking the error in re-solving opt-out values into separate underestimation and overestimation terms. The first part of this proof is a bound that takes into account the re-solving solution quality, and how much the average values underestimate the best response to the average. This underestimation is bounded by the opponent regret at a subgame, which requires the solving algorithm to have low regret everywhere in the game: low regret for the opponent does not directly imply that the opponent has low regret in portions of the game that they do not play. The second part of the proof is placing a bound on the overestimation, using the player's regret rather than the opponent's regret.

We start by noting that from the opponent player  $o$ 's point of view, we can replace an information set  $s_o$  with a terminal that has utility  $BV^{\bar{\pi}}(s_o)$ , and the best response utility  $BV_o^{\bar{\pi}, s_o \leftarrow BV^{\bar{\pi}}(s_o)}$  in this modified game will be equal to  $BV_o^{\bar{\pi}}$ . We can extend this to the entire subgame  $S$ , replacing each  $s_o$  with a terminal giving the opponent the best response value:  $BV_o^{\bar{\pi}, S \leftarrow BV^{\bar{\pi}}(S)} = BV_o^{\bar{\pi}}$ . Using this notation, we can rewrite  $BV_o^{\bar{\pi} \leftarrow \pi^S}$ :

$$\begin{aligned} & BV_o^{\bar{\pi} \leftarrow \pi^S} - BV_o^{\bar{\pi}} \\ &= BV_o^{\bar{\pi}, S \leftarrow BV^{\pi^S}(S)} - BV_o^{\bar{\pi}} \end{aligned}$$

Next, note that  $BV^{\pi^S}(s_o)$ , the opponent's counterfactual best response to the re-solved subgame strategy  $\pi^S$  at any  $s_o$  at the root of  $S$ , is no greater than the value of  $\max\{BV^{\pi^S}(s_o), \bar{v}(s_o)\}$ , the value of  $s_o$  within the re-solving game before the gadget where the opponent has decision to opt-out for a fixed value  $\bar{v}(s_o)$ . That is, adding an extra opponent action which terminates the game never decreases the opponent's best response utility. Extending this to the entire subgame  $S$  again, we get

$$\begin{aligned} & BV_o^{\bar{\pi}, S \leftarrow BV^{\pi^S}(S)} - BV_o^{\bar{\pi}} \\ & \leq BV_o^{\bar{\pi}, S \leftarrow \max\{BV^{\pi^S}(S), \bar{v}\}} - BV_o^{\bar{\pi}} \end{aligned} \tag{2}$$

From Lemma 1 of [55], the game value of a re-solving game with opt-out values  $\bar{v}(s_o)$  is  $U_{\bar{v}, \bar{\pi}}^S + \sum_{s_o \in \mathcal{S}_o(s_{\text{pub}})} \bar{v}(s_o)$ , for some underestimation error on the opt-out values that is given by

$$U_{\bar{v}, \bar{\pi}}^S := \min_{\pi^*} \sum_{s_o \in \mathcal{S}_o(s_{\text{pub}})} (BV^{\bar{\pi} \leftarrow \pi^*}(s_o) - \bar{v}(s_o))^+$$

Given the re-solving regrets, we have  $BV_o^{\pi^S} \leq (\bar{R}_o^S)^+ + (\bar{R}_i^S)^+ + U_{\bar{v}, \bar{\pi}}^S + \sum_{s_o \in \mathcal{S}_o(s_{\text{pub}})} \bar{v}(s_o)$ . Because  $BV_o^{\bar{\pi}, s_o \leftarrow w + \epsilon} \leq BV_o^{\bar{\pi}, s_o \leftarrow w} + \epsilon$  for  $\epsilon \geq 0$ , we can use this inequality to update Equation 2. That is, there is some component-wise non-negative vector  $\epsilon$  such that  $BV^{\pi^S}(\tilde{S}) = \bar{v}(\cdot) + \epsilon$  and  $\epsilon \cdot \mathbf{1} \leq (\bar{R}_o^S)^+ + (\bar{R}_i^S)^+ + U_{\bar{v}, \bar{\pi}}^S$ , so that

$$\begin{aligned} & BV_o^{\bar{\pi}, S \leftarrow \max\{BV^{\pi^S}(S), \bar{v}\}} - BV_o^{\bar{\pi}} \\ &= BV_o^{\bar{\pi}, S \leftarrow \bar{v} + \epsilon} - BV_o^{\bar{\pi}} \\ &\leq BV_o^{\bar{\pi}, S \leftarrow \bar{v}} + \epsilon \cdot \mathbf{1} - BV_o^{\bar{\pi}} \\ &\leq BV_o^{\bar{\pi}, S \leftarrow \bar{v}} + (\bar{R}_o^S)^+ + (\bar{R}_i^S)^+ + U_{\bar{v}, \bar{\pi}}^S - BV_o^{\bar{\pi}} \end{aligned} \tag{3}$$

Looking at  $U_{\bar{v}, \bar{\pi}}^S$ , we note that this minimum is no greater than the case when  $\pi^* = \bar{\pi}$ . The difference  $BV^{\bar{\pi} \leftarrow \pi^*}(s_o) - \bar{v}(s_o)$  is the average full counterfactual regret  $R_{s_o}$  of strategy  $\bar{\pi}$  at  $s_o$ . Restricting our attention to  $\mathcal{L}_{s_{\text{pub}}}^t$ , the portion of the lookahead tree restricted to  $s_{\text{pub}}$  and its descendants, Theorem 3 gives us a bound on  $U_{\bar{v}, \bar{\pi}}^S$  and we can update Equation 3

$$\begin{aligned} & BV_o^{\bar{\pi}, S \leftarrow \bar{v}} + (\bar{R}_o^S)^+ + (\bar{R}_i^S)^+ + U_{\bar{v}, \bar{\pi}}^S - BV_o^{\bar{\pi}} \\ &\leq BV_o^{\bar{\pi}, S \leftarrow \bar{v}} - BV_o^{\bar{\pi}} \\ &\quad + (\bar{R}_o^S)^+ + (\bar{R}_i^S)^+ \max_t |\mathcal{F}(\mathcal{L}_{s_{\text{pub}}}^t)|(\epsilon + \xi) + \sum_{s_{\text{pub}} \in \mathcal{N}(\mathcal{L}_{s_{\text{pub}}}^T)} |\mathcal{S}_i(s_{\text{pub}})| U \sqrt{\frac{A}{T}} \end{aligned} \tag{4}$$

Looking at just the difference in opponent counterfactual best response values, we can again get an upper bound by giving the opponent the choice at all information sets at the root of subgame  $S$

of playing a best response against the unmodified strategy  $\bar{\pi}$  to get value  $BV^{\bar{\pi}}(S)$ , or opting out to get value  $\bar{v}$ .

$$\begin{aligned}
& BV_o^{\bar{\pi}, S \leftarrow \bar{v}} - BV_o^{\bar{\pi}} \\
& \leq BV_o^{\bar{\pi}, S \leftarrow \max\{BV^{\bar{\pi}}(S), \bar{v}\}} - BV_o^{\bar{\pi}} \\
& = (BV_o^{\bar{\pi}, S \leftarrow \max\{BV^{\bar{\pi}}(S), \bar{v}\}} - \bar{v}_o) - (BV_o^{\bar{\pi}} - \bar{v}_o) \\
& \leq (BV_o^{\bar{\pi}, S \leftarrow \max\{BV^{\bar{\pi}}(S), \bar{v}\}} - \bar{v}_o) - (BV_o^{\pi^*} - \bar{v}_o) \\
& = (BV_o^{\bar{\pi}, S \leftarrow \max\{BV^{\bar{\pi}}(S), \bar{v}\}} - \bar{v}_o) - (v_o^{\pi^*} - \bar{v}_o) \\
& = (BV_o^{\bar{\pi}, S \leftarrow \max\{BV^{\bar{\pi}}(S), \bar{v}\}} - \bar{v}_o) + (v_i^{\pi^*} - \bar{v}_i) \\
& \leq (BV_o^{\bar{\pi}, S \leftarrow \max\{BV^{\bar{\pi}}(S), \bar{v}\}} - \bar{v}_o) + (BV_i^{\bar{\pi}} - \bar{v}_i) \\
& = (BV_o^{\bar{\pi}, S \leftarrow \max\{BV^{\bar{\pi}}(S), \bar{v}\}} - \bar{v}_o) + \bar{R}_i
\end{aligned} \tag{5}$$

The difference of the first two terms is the regret in the opt-out game described above, where we have lifted each iteration strategy  $\pi^t$  into this game by never selecting the opt-out choice. Consider the immediate counterfactual regret  $\tilde{R}^T(s_o)$  in this situation for any information state  $s_o$  in this augmented game. Writing this in terms of the original immediate counterfactual regret  $R^T(s_o)$  and the opt-out value, we get

$$\begin{aligned}
\tilde{R}^T(s_o) &= \max\{T(\bar{v}[s_o] - \bar{v}[s_o]), R^T(s_o)\} \\
&= (R^T(s_o))^+
\end{aligned}$$

Because the positive immediate regret in the opt-out game is the same as the positive regret in the original game, we can use the Theorem 3 bound, which is composed from immediate regrets. Putting this together with Equation 4 and Equation 5, we get

$$\begin{aligned}
& BV_o^{\bar{\pi} \leftarrow \pi^S} - BV_o^{\bar{\pi}} \\
& \leq (\bar{R}_o^S)^+ + (\bar{R}_i^S)^+ + \bar{R}_i \\
& \quad + 2(\max_t |\mathcal{F}(\mathcal{L}_{s_{\text{pub}}}^t)|(\epsilon + \xi) + \sum_{s_{\text{pub}} \in \mathcal{N}(\mathcal{L}_{s_{\text{pub}}}^T)} |\mathcal{S}_i(s_{\text{pub}})|U\sqrt{\frac{A}{T}})
\end{aligned}$$

□

## Continual Re-solving

Continual re-solving puts GT-CFR together with re-solving the previously solved subgame. A bound on final solution quality then follows directly from applications of Theorem 3 and Theorem 4.

**Theorem 5.** *Assume we have played a game using continual re-solving, with one initial solve and  $D$  re-solving steps. Each solving or re-solving step finds an approximate Nash equilibrium through  $T$  iterations of GT-CFR using a value function with quality  $\epsilon, \xi$ , public states are never removed from the lookahead tree, the maximum interior size  $\sum_{s_{\text{pub}} \in \mathcal{N}(\mathcal{L}^T)} |\mathcal{S}_i(s_{\text{pub}})|$  of all lookahead trees is bounded by  $N$ , the sum of frontier sizes across all lookahead trees is bounded by  $F$ , the maximum number of actions at any information sets is  $A$ , and the maximum difference in values between any two strategies is  $U$ . The exploitability of the final strategy is then bounded by  $(5D + 2) \left( F(\epsilon + \xi) + NU\sqrt{\frac{A}{T}} \right)$ .*

*Proof.* The exploitability  $\text{EXP}_0$  of the player's initial strategy from the original solve is bounded by the sum of the regrets for both players. Theorem 3 provides regret bounds for GT-CFR, so

$$\text{EXP}_0 \leq 2 \left( F(\epsilon + \xi) + NU\sqrt{\frac{A}{T}} \right)$$

Each subsequent re-solve is operating on the strategy of the previous step, using the average values for the opt-out values. That is, the first re-solve will be updating the strategy from the initial solve, the second re-solve will be updating the subgame strategy from the first re-solve, and so on.

Theorem 4 provides a bound on how much the exploitability increases after each re-solving step, with Theorem 3 providing the necessary regret bounds

$$\begin{aligned}\text{EXP}_d &\leq \text{EXP}_{d-1} + (\bar{R}_o^S)^+ + (\bar{R}_i^S)^+ + \bar{R}_i + 2 \left( F(\epsilon + \xi) + NU \sqrt{\frac{A}{T}} \right) \\ &\leq \text{EXP}_{d-1} + 5 \left( F(\epsilon + \xi) + NU \sqrt{\frac{A}{T}} \right)\end{aligned}$$

Unrolling for  $D$  re-solving steps leads to the final bound.  $\square$